0026-895X/10/7704-575–592$20.00
MOLECULAR PHARMACOLOGY
Copyright © 2010 The American Society for Pharmacology and Experimental Therapeutics
Mol Pharmacol 77:575–592, 2010

Vol. 77, No. 4
61259/3570751
Printed in U.S.A.

Hepatic Heme-Regulated Inhibitor (HRI) Eukaryotic Initiation Factor 2α Kinase: A Protagonist of Heme-Mediated Translational Control of CYP2B Enzymes and a Modulator of Basal Endoplasmic Reticulum Stress Tone

Poulomi Acharya, Jane-Jane Chen, and Maria Almira Correia

Departments of Cellular & Molecular Pharmacology (P.A., M.A.C.), Pharmaceutical Chemistry (M.A.C.), Biopharmaceutical Sciences (M.A.C.), and the Liver Center (P.A., M.A.C.), University of California, San Francisco, California; and Harvard-Massachusetts Institute of Technology Division of Health Sciences and Technology, Massachusetts Institute of Technology, Cambridge, Massachusetts (J.-J.C.)

Received September 25, 2009; accepted January 12, 2010

ABSTRACT

We have reported previously that the hepatic heme-regulated inhibitor (HRI)-eukaryotic initiation factor 2α (eIF2α) kinase is activated in acute heme-deficient states, resulting in translational shut-off of global hepatic protein synthesis, including phenobarbital (PB)-mediated induction of CYP2B enzymes in rats. These findings revealed that heme regulates hepatic CYP2B synthesis at the translational level via HRI. As a proof of concept, we have now employed a genetic HRI-knockout (KO) mouse hepatocyte model. In HRI-KO hepatocytes, PB-mediated CYP2B protein induction is no longer regulated by hepatic heme availability and proceeds undeterred even after acute hepatic heme depletion. It is noteworthy that genetic ablation of HRI led to a small albeit significant elevation of basal hepatic endoplasmic reticulum (ER) stress as revealed by the activation of ER stress-inducible RNA-dependent protein kinase-like ER-integral (PERK) eIF2α-kinase, and induction of hepatic protein ubiquitination and ER chaperones Grp78 and Grp94. Such ER stress was further augmented after PB-mediated hepatic protein induction. These findings suggest that HRI normally modulates the basal hepatic ER stress tone. Furthermore, because HRI exists in both human and rat liver in its heme-sensitive form and is inducible by cytochrome P450 inducers such as PB, these findings are clinically relevant to acute heme-deficient states, such as the acute hepatic porphyrias. Activation of this exquisitely sensitive heme sensor would normally protect cells by safeguarding cellular energy and nutrients during acute heme deficiency. However, similar HRI activation in genetically predisposed persons could lead to global translational arrest of physiologically relevant enzymes and proteins, resulting in the severe and often fatal clinical symptoms of the acute hepatic porphyrias.

Suppression of global protein synthesis through translational control is an effective way to preserve cellular energy and nutrients after various forms of cellular stress and injury. Through a rapid and reversible control of gene expression, it critically regulates various vital cellular processes, including growth stimulation, cell cycle progression, differentiation, hypoxia, ER stress, and heme deficiency (Chen, 2000, 2007; Harding et al., 2002, 2003; Zhang et al., 2002a,b; Kaufman, 2004; Scheuner et al., 2006; Wek et al., 2006). In these instances, this control is exerted at the initiation of translation through Ser51-phosphorylation of the α-subunit of the eukaryotic initiation factor (eIF2α). Productive translational initiation requires GTP-bound eIF2 that upon GTP hydrolysis before protein chain elon-

These studies were supported by the National Institutes of Health National Institute of Diabetes and Digestive and Kidney Diseases [Grants DK26506 (to M.A.C.), DK016272, DK078442 (to J.-J.C.)]. We also acknowledge the UCSF Liver Center Core on Cell and Tissue Biology supported by the National Institutes of Health National Institute of Diabetes and Digestive and Kidney Diseases [Grant P30-DK26743].

Article, publication date, and citation information can be found at http://molpharm.aspetjournals.org.

doi:10.1124/mol.109.061259.

ABBREVIATIONS: ER, endoplasmic reticulum; eIF2α, α-subunit of the eukaryotic initiation factor eIF2; eIF2αP, phosphorylated eIF2α; PKR, RNA-dependent protein kinase; PERK, PKR-like ER-bound eIF2α-kinase; GCN2, general control nonderepressible-2 eIF2α kinase; PAGE, polyacrylamide gel electrophoresis; BSA, bovine serum albumin; HRI, heme-regulated inhibitor; PB, phenobarbital; Dex, dexamethasone; BSA, bovine serum albumin; DMSO, dimethyl sulfoxide; WT, wild type; KO, knockout; MGB, mixed genetic background; TDO, tryptophan 2,3-dioxygenase; qRT-PCR, Quantitative real time polymerase chain reaction; HRI-P, 92-kDa phosphorylated HRI species; MG132, *N*-benzoyloxycarbonyl (*Z*)-Leu-Leu-leucinal.

gation is converted to GDP-bound eIF2. Fresh translational initiation cycles require GDP exchange with GTP catalyzed by the relatively scanty eIF2B. The enhanced affinity of phosphorylated eIF2α (eIF2αP) for eIF2B results in its sequestration in an inactive GDP-eIF2-eIF2B complex. This sequestration prevents eIF2B-catalyzed GDP-GTP exchange and consequent regeneration of GTP-eIF2 for fresh initiation cycles (Chen, 2000; Harding et al., 2002; Zhang et al., 2002a,b; Wek et al., 2006), resulting in translational shut off of global protein synthesis.

In mammalian cells, eIF2α phosphorylation is catalyzed by four distinct eIF2α kinases: double-stranded RNA/interferon-inducible PKR [RNA-dependent protein kinase (EIF2AK2)], the ER stress-inducible PERK [PKR-like ER kinase (EIF2AK3)], amino acid deprivation- and UV-irradiation-inducible GCN2 [general control nonderepressible-2 (EIF2AK4)], and HRI [the heme-regulated inhibitor (EIF2AK1)] activated by heme deficiency (Chen, 2000; Harding et al., 2002; Zhang et al., 2002a,b; Scheuner et al., 2006; Wek et al., 2006). In erythroid cells, HRI plays a critical role in hemoglobin synthesis through coordinated regulation of the synthesis of its heme and globin moieties (Han et al., 2001; Chen, 2007). Although HRI eIF2α kinase was once viewed as erythroid-specific (Pal et al., 1991; Chen et al., 1994; Crosby et al., 1994; Chen, 2000), the existence of HRI mRNA in nonerythroid tissues and the characterization of a mouse liver HRI protein have been reported (Delaunay et al., 1977; Mellor et al., 1994; Berlanga et al., 1998; Igarashi et al., 2004). However, a plausible reason for overlooking HRI in the liver is its apparently low abundance (per milligram of protein) relative to erythroid HRI. Thus, although erythroid protein

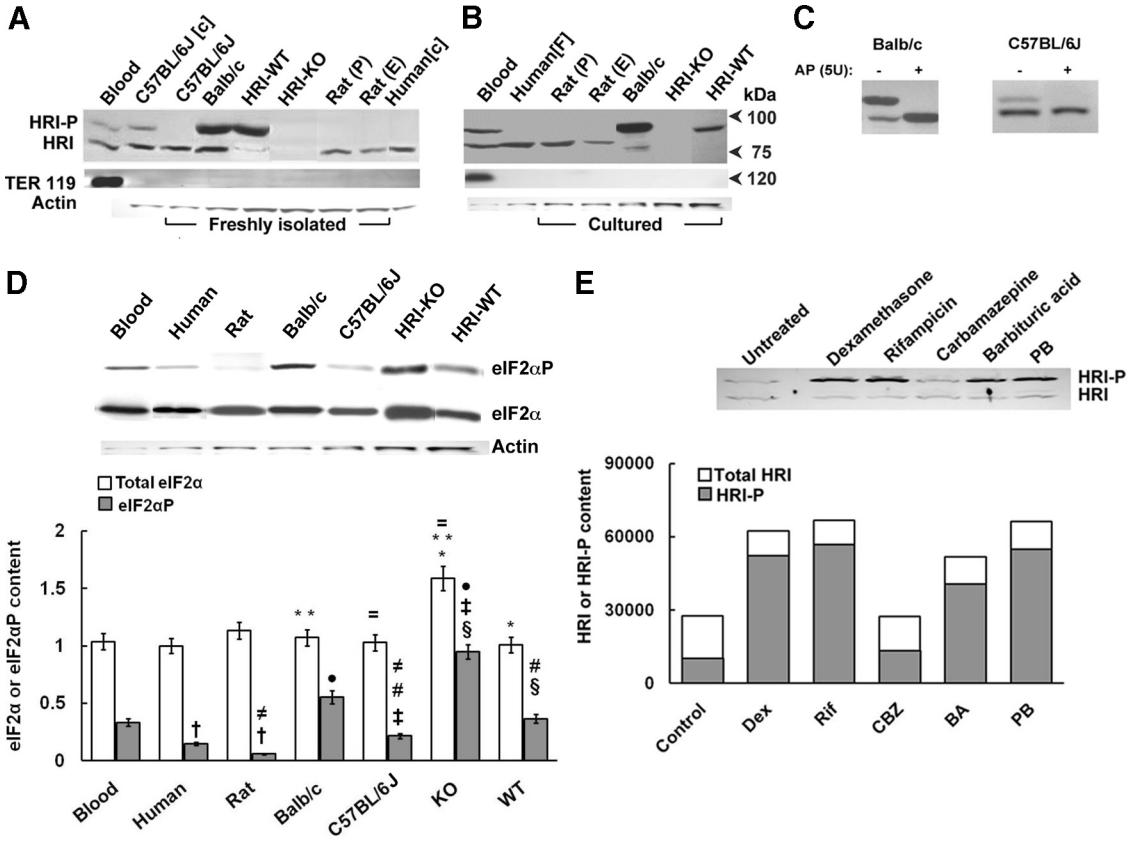

Fig. 1. Immunoblotting analyses of HRI content in freshly isolated and cultured human, rat, and mouse hepatocytes. A, hepatocytes from human, rat and mouse [C57BL/6J, BALB/c, MGB HRI (+/+; WT), or HRI (−/−; KO] were size-fractionated by elutriation (E) or Percoll sedimentation (P) and then lysed either as freshly isolated cells (F) or after culture [c] as detailed under *Materials and Methods*). Hepatocyte lysates (100 μg of protein) were subjected to Western immunoblotting analyses of HRI and TER-119 content as described under *Materials and Methods*. Mouse blood lysates (10 μg of protein) containing mature erythroid cells were immunoblotted in parallel as positive controls for both HRI as well as erythroid (TER-119) contamination. A representative example of Western immunoblotting analyses is shown at the top, with corresponding aliquots used for actin immunoblotting analyses as loading controls. B, a representative example of HRI and TER119 Western immunoblotting analyses of lysates (100 μg of protein) from cultured hepatocytes, lysates from mouse blood (20 μg of protein), and freshly isolated human hepatocytes (100 μg of protein as in A) is shown at the top with corresponding aliquots used for actin immunoblotting analyses as loading controls at the very bottom. Native nonphosphorylated HRI and autophosphorylated HRI species are usually detected at ≈76 and 92 kDa, respectively. Note the species differences in actin content of 10 μg of hepatocyte lysate protein. C, lysates (100 μg of protein) from freshly isolated BALB/c or C57BL/6J mouse hepatocytes (10^6 cells) were incubated in vitro with or without alkaline phosphatase at 37°C for 1 h (Lu et al., 2001), and then subjected to HRI immunoblotting analyses as described previously (*Materials and Methods*). D, determination of the relative constitutive total hepatic eIF2α and eIF2αP content in lysates (10 μg of protein) of cultured hepatocytes or freshly isolated mouse blood (10 μg of protein) as shown in A and B above. A representative example of Western immunoblotting analyses is shown at the top with corresponding aliquots (10 μg of protein) used for actin immunoblotting analyses as loading controls. Densitometric quantification of total hepatic eIF2α and eIF2αP content and corresponding statistically significant differences between values (mean ± S.D.) from three individual experiments are shown at the bottom. Statistically significant differences in total hepatic eIF2α or eIF2αP content were observed between the two mean ± S.D. values each marked with the same symbol as follows: *, $p < 0.001$; **, $p < 0.001$; =, $p < 0.001$; §, $p < 0.001$; ‡, $p < 0.001$; ●, $p < 0.001$; †, $p < 0.05$; #, $p < 0.05$; and ≠, $p < 0.05$. E, induction of hepatic HRI protein content by Dex (100 μM), PB (500 μM), rifampin (Rif; 15 μM), carbamazepine (CBZ; 500 μM), barbituric acid (BA; 5 mM). Cell cultures were treated with each of the above agents for 2 days, included daily in cell culture media. A prototype immunoblot of hepatocyte lysates (50 μg of protein) is shown on top, with the average protein normalized densitometric quantitation from two separate experiments shown at the bottom.

synthesis is predominantly committed to hemoglobin production, hepatic protein synthesis is not only far more diverse but also much more prolific in yield. Thus immunochemical detection of hepatic HRI within this enormous intracellular protein background requires very high protein amounts, highly specific/immunoreactive antibodies, and highly sensitive detection systems. Indeed, these improved approaches have enabled us to document the existence of a heme-sensitive 76-kDa HRI protein

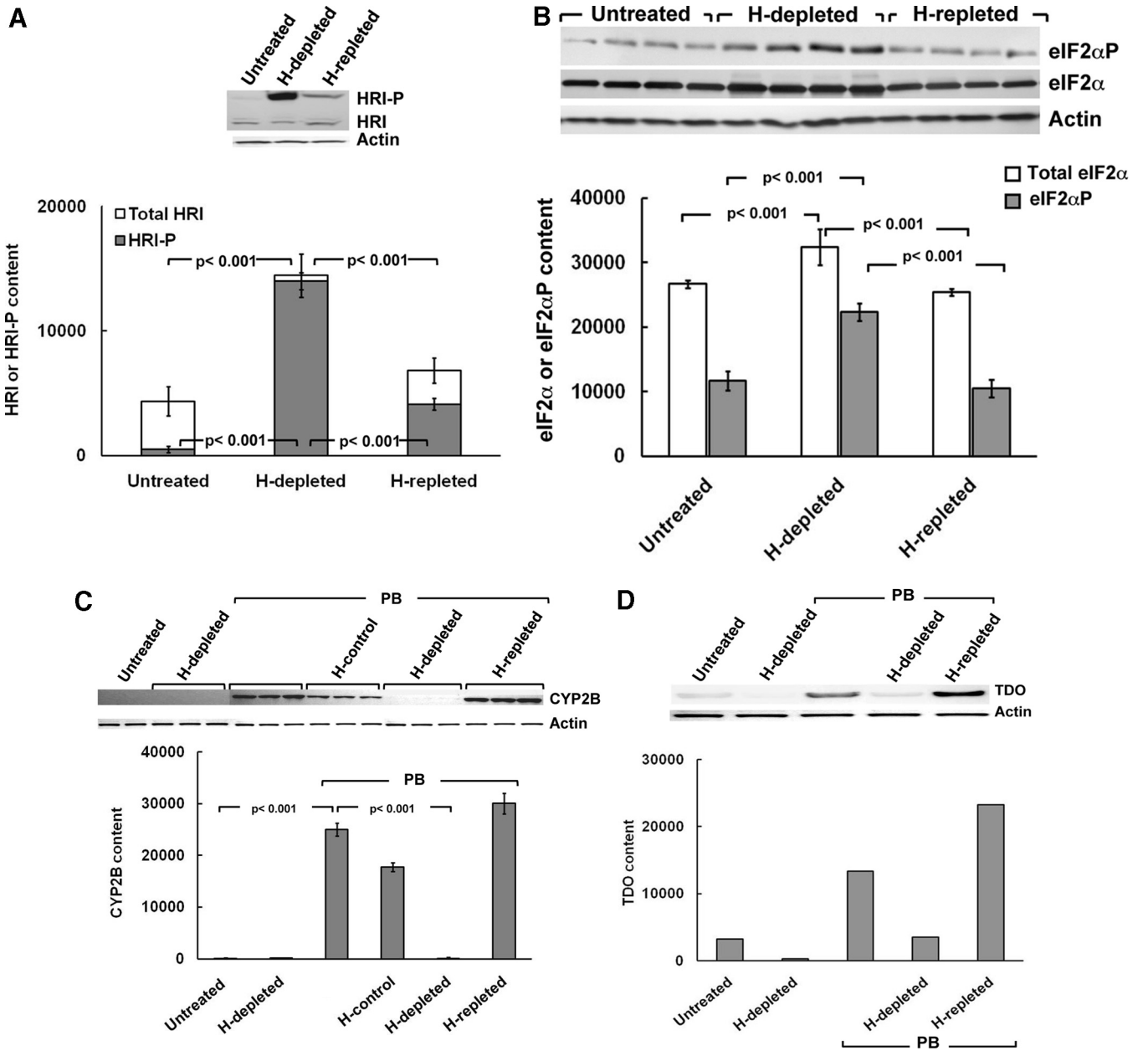

Fig. 2. Effects of acute hepatic heme depletion and repletion on hepatic HRI autophosphorylation, eIF2α kinase activation, and PB-mediated CYP2B induction in cultured C57BL/6J mouse hepatocytes. Mouse hepatocyte cultures were untreated, heme (H)-depleted, or heme-repleted after heme depletion as detailed under *Materials and Methods*. A, a representative example of HRI Western immunoblotting analyses of these hepatocyte lysates (100 μg of protein) is shown at the top, with corresponding aliquots used for actin immunoblotting analyses as loading controls. Densitometric quantification of total hepatic HRI and autophosphorylated HRI (HRI-P) content and corresponding statistically significant differences between mean ± S.D. of three individual experiments are shown at the bottom. B, Western immunoblotting analyses of total eIF2α and eIF2αP content in these hepatocyte lysates (10 μg of protein) is shown at the top, with corresponding aliquots used for actin immunoblotting analyses as loading controls. Densitometric quantification of total hepatic eIF2α and eIF2αP content, and corresponding statistically significant differences between mean ± S.D. of 4 individual experiments are shown at the bottom. C, mouse hepatocyte cultures were untreated (first two lanes) or heme-depleted (H; next three lanes), pretreated with PB (next 12 lanes): alone (PB), with heme (H-control), heme depletion (H-depleted), or heme repletion after heme depletion (H-repleted), as detailed under *Materials and Methods*. CYP2B Western immunoblotting analyses of these hepatocyte lysates (30 μg of protein) is shown at the top, with corresponding aliquots used for actin immunoblotting analyses as loading controls. Densitometric quantification of hepatic CYP2B content from three individual experiments is shown at the bottom. Statistical analyses revealed significant differences in hepatic CYP2B content between untreated and PB-pretreated at $p < 0.001$, PB/H-depleted, and PB-pretreated at $p < 0.001$, PB/H-repleted, and PB/H-depleted at $p < 0.001$. No statistically significant differences were observed between PB-pretreated and PB/H-repleted. D, mouse hepatocyte cultures were treated as in C. TDO Western immunoblotting analyses of these hepatocyte lysates (20 μg of protein) is shown at the top, with corresponding aliquots used for actin immunoblotting analyses as loading controls. Densitometric quantification of hepatic TDO content as the average values from 2 individual experiments is shown at the bottom.

in cultured rat hepatocytes (Liao et al., 2007). Through a combination of approaches including cloning, heterologous expression, isolation, purification, immunoblotting, immunoaffinity capture, and proteomic analyses we have identified it as a bona fide HRI that is activated via autophosphorylation by acute hepatic heme depletion, resulting in global protein translational shutoff, and functionally inhibited by heme repletion (Han et al., 2005b; Liao et al., 2007). Accordingly, in heme-depleted rat hepatocytes, the de novo syntheses (determined by [^{35}S]Met/Cys-incorporation into immunoprecipitable protein) of the phenobarbital (PB)-inducible CYP2B enzymes (Han et al., 2005b) and dexamethasone (Dex)-inducible tryptophan 2,3-dioxygenase (TDO; Liao et al., 2007) were greatly impaired in a heme-reversible manner. To directly verify the role of hepatic HRI in the translational shutoff of PB-inducible CYP2B enzymes, we have used a HRI gene knockout mouse model [HRI(−/−)] (Han et al., 2001). Our findings described in this report reveal that genetic ablation of HRI abrogates the heme deficiency-induced impairment of hepatic PB-inducible CYP2B and CYP3A synthesis, thereby providing proof for its role in this process. We also document herein that hepatic HRI is not only PB-inducible but also exists in human hepatocytes. Thus in acute heme deficiency, its heme-sensing function would be normally protective, conserving cellular energy and nutrients. However, in acute heme-deficient states, clinically known as the acute hepatic porphyrias, its translational arrest of physiologically relevant proteins could also contribute to the symptoms of these hepatic diseases in persons who are genetically predisposed.

We find it equally intriguing that HRI plays a role in containing basal levels of ER-stress. HRI(−/−) hepatocytes exhibit not only significantly elevated constitutive PERK activation but also significantly enhanced levels of eIF2αP, ubiquitinated proteins, and ER stress chaperones than the corresponding wild-type cells. The latter findings reveal that HRI may modulate the basal hepatocellular stress tone through its intrinsic functional capacity as a heme sensor.

Materials and Methods

Materials. Common cell culture medium and supplements such as Williams' Medium E, insulin-transferrin-selenium-G (100×), bovine serum albumin (BSA), penicillin/streptomycin, L-glutamine, liver digestion medium, and liver perfusion medium were obtained from Invitrogen (Carlsbad, CA). Collagen type I was prepared from frozen rat tails according to a protocol established by the UCSF Liver Center Cell and Tissue Biology Core Facility. Matrigel was obtained from BD Biosciences Discovery Labware (Bedford, MA). Petri dishes (60 mm; Permanox) were purchased from Nalge Nunc International (Rochester, NY). Phenylmethylsulfonyl fluoride, E-64, calf intestinal alkaline phosphatase (10,000 units/ml), and Dex were purchased from Sigma/Aldrich (St. Louis, MO). Sodium vanadate, β-glycerophosphate, and sodium fluoride were obtained from Thermo Fisher Scientific (Waltham, MA). Leupeptin was purchased from Roche Applied Science (Indianapolis, IN); aprotinin, pepstatin A, and bestatin were obtained from MP Biomedicals LLC (Solon, OH). 4-(2-Aminoethyl)benzenesulfonyl fluoride hydrochloride was purchased from Alexis Biochemicals (San Diego, CA). Rabbit polyclonal immunoglobulins G were raised commercially against purified recombinant rat hepatic eIF2α kinase (HRI), and purified by Hi-Trap Protein A-Sepharose affinity chromatography. TER119 antibody was purchased from eBioscience (San Diego, CA).

Rats. Male Sprague-Dawley rats (4–6 weeks old) were purchased from Simonsen Laboratories (Gilroy, CA). Animals were housed at the University of California San Francisco Animal Care Facility, fed and given water ad libitum, and handled according to Institutional Animal Care and Use Committee guidelines.

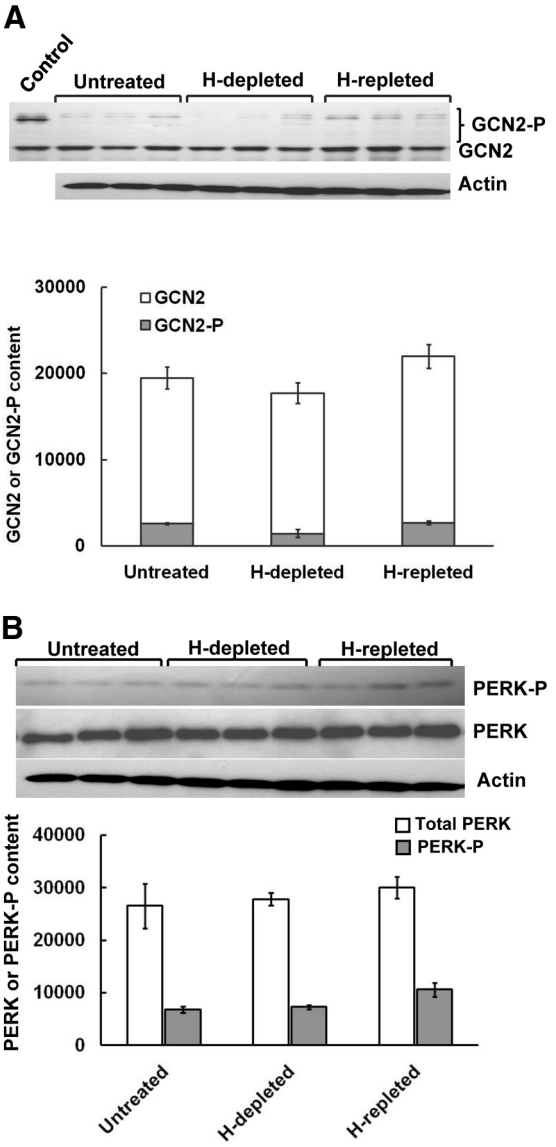

Fig. 3. Effects of acute hepatic heme depletion and repletion on hepatic content of GCN2 and PERK, and their autophosphorylated species in cultured C57BL/6J mouse hepatocyes. A, mouse hepatocyte cultures were untreated, heme (H)-depleted, or heme-repleted after heme depletion as detailed under *Materials and Methods*. A, GCN2 and GCN2-P Western immunoblotting analyses of these hepatocyte lysates (50 μg of protein) are shown at the top, with corresponding aliquots used for actin immunoblotting analyses as loading controls. Lysates (250 ng of GCN2 protein) from HeLa cells overexpressing GCN2 were included as a positive control (Control). Densitometric quantification of total hepatic GCN2 and autophosphorylated GCN2 (GCN2-P) content (mean ± S.D.) of three individual experiments is shown at the bottom. No statistically significant differences between any of these treatments in either total GCN2 (GCN2 + GCN2-P) or GCN2-P content were found. B, PERK and PERK-P Western immunoblotting analyses of these hepatocyte lysates (100 μg of protein) are shown at the top, with corresponding aliquots used for actin immunoblotting analyses as loading controls. The densitometric quantification of the relative PERK-P content (solid bars) to the total immunochemically detectable PERK content (open bars) is shown at the bottom. Values represent mean ± S.D. of the same three separate experiments shown in A. No statistically significant differences between any of these treatments in either PERK or PERK-P content were found. In parallel, smaller aliquots (10 μg of protein) of these same SDS-PAGE sample buffer-solubilized cell lysates were subjected to actin immunoblotting analyses.

Hepatocyte Isolation and Culture. Hepatocytes were isolated from rats by in situ liver perfusion with collagenase (liver digest medium) and purified by centrifugal elutriation. Hepatocytes (3×10^6) were seeded onto 60-mm Permanox culture dishes precoated with type I rat tail collagen. Cells were cultured as described previously (Han et al., 2005b; Faouzi et al., 2007) in Williams E medium containing insulin-transferrin-selenium G, 0.1 μM Dex, 50 U/ml penicillin/streptomycin, 2 mM L-glutamine, and 0.1% BSA. Cells were overlaid with 0.25 mg/ml Matrigel 3 h after plating. Cells were maintained for 2 days with a daily change of medium to enable recovery and hepatic function restoration (LeCluyse et al., 1999). Treatments were initiated at 72 h of culture. Cells were treated with vehicle (DMSO) or 3,5-dicarbethoxy-2,6-dimethyl-4-ethyl-1,4-dihydropyridine (30 μM) + *N*-methylprotoporphyrin (50 μM) for 1 h to deplete hepatic heme. At this time (73 h), some cell cultures were repleted with hemin [dissolved in DMSO and complexed with BSA (1:2)], added in four divided aliquots at 6 h intervals, totaling hemin (20 μM, final concentration) (H-repleted). Others received just the corresponding volume of DMSO/BSA solution and served as the heme-depleted (H-depleted) cultures. In some experiments in which the effects of PB were examined, the drug (1 mM) was added 1 h after heme depletion and followed either with or without hemin. Controls with PB alone were also included.

At 96 h, cells were harvested in lysis buffer consisting of Tris-HCl (20 mM, pH 7.5), 1% Triton, NaCl (150 mM), 10% glycerol, EDTA (1 mM), EGTA (1 mM), NaF (100 mM), tetrabasic sodium pyrophosphate (10 mM), β-glycerophosphate (17.5 mM), *N*-ethylmaleimide (5 mM), Na_3VO_4 (1 mM) and protease inhibitors phenylmethylsulfonyl fluoride (1 mM), leupeptin (20 μM), aprotinin (1.5 μM), E-64 (50 μM), pepstatin (10 μM), antipain (10 μM), 4-(2-aminoethyl)benzenesulfonyl fluoride hydrochloride (1 mM), and bestatin (60 μM). The cells were lysed using an Omni-TH homogenizer (Omni International, Kennesaw, GA) and sonicated for 40 s. Lysates were clarified by sedimentation at maximum speed in a tabletop microcentrifuge at 4°C for 15 min. Lysate supernatants were subjected to Western immunoblotting analyses and densitometric quantification using ImageJ software (http://rsbweb.nih.gov/ij/).

Human Hepatocyte Cultures. Freshly isolated hepatocytes were obtained from CellzDirect (Durham, NC). After a Percoll (GE Healthcare, Chalfont St. Giles, Buckinghamshire, UK) centrifugation to exclude nonviable cells, they were cultured exactly as described above for cultured rat hepatocytes. On the fifth day of culture, cells were lysed and processed exactly as described for rat hepatocyte cultures.

Mouse Hepatocyte Cultures. C57BL/6J and BALB/c mice were purchased from Simonsen Laboratories (Gilroy, CA), and housed for 2 to 3 days with food and water until acclimatized. Transgenic HRI (+/+; WT) and HRI (−/−; KO) mice of an inbred mixed C57BL/6J and S129 genetic background (MGB) were generated and genotyped exactly as described previously (Han et al., 2001). HRI (−/−) mice in pure C57BL/6J background were generated by backcrossing the MGB mice with C57BL/6J mice for 10 generations and similarly genotyped. Hepatocytes were isolated by collagenase perfusion as described above from two mouse livers of each strain, pooled for each individual experiment and purified by Percoll-gradient centrifugation. They were cultured, treated and harvested exactly as described for rat hepatocytes.

Pulse-Chase Analyses. The experimental details of the pulse-chase along with subsequent CYP2B immunoprecipitation, scintillation counting and Typhoon 9400 variable mode imager (GE Healthcare) analyses of CYP2B immunoprecipitates were exactly as described previously (Han et al., 2005b).

Immunoblotting Analyses. Unless otherwise indicated, 5% nonfat milk in 0.1% Tris-buffered saline/Tween 20 was used for blocking and to make all primary and secondary antibody dilutions. All immunoblots were developed with the SuperSignal West maximum sensitivity Femto or Pico chemiluminescent substrate from Pierce (Rockford, IL). Actin immunoblotting analyses were routinely conducted with each lysate to insure equivalent protein loading. However, because of the low abundance of basal hepatic PERK, GCN2, and HRI protein content, the protein amounts required for their detection even by the maximum sensitivity Femto system greatly exceeded those required for the detection of the relatively more abundant actin protein. The immunoblots were therefore loaded on

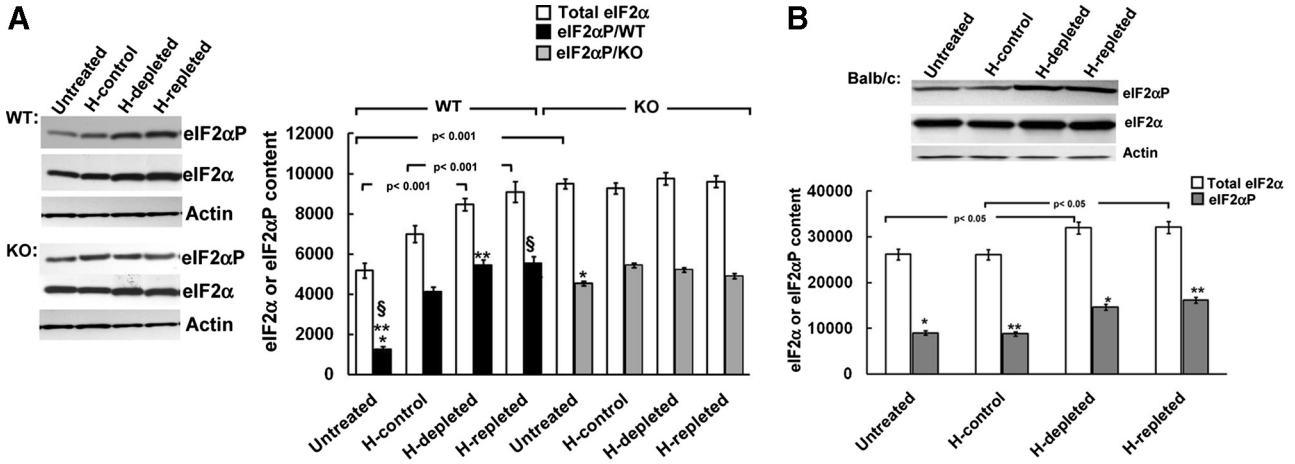

Fig. 4. Effects of acute hepatic heme depletion and repletion on hepatic eIF2α kinase activity in cultured MGB wild-type [WT; HRI (+/+)] and HRI knockout [KO; HRI (−/−)] mouse hepatocytes. A, WT or KO mouse hepatocyte cultures were untreated, treated with heme (20 μM; H-control), heme-depleted, or heme-repleted after heme depletion, as detailed under *Materials and Methods*. A representative example of total eIF2α and eIF2αP Western immunoblotting analyses of these hepatocyte lysates (10 μg of protein) is shown on the left, with corresponding aliquots used for actin immunoblotting analyses as loading controls. Densitometric quantification of total hepatic eIF2α and eIF2αP content and corresponding statistically significant differences between mean ± S.D. of three individual experiments are shown on the right. Statistically significant differences were observed between basal eIF2αP content of untreated WT and KO hepatocytes (*) at $p < 0.001$ and between that of untreated WT and either WT/H-depleted (**) or WT/H-repleted (§) at $p < 0.001$. B, BALB/c mouse hepatocyte cultures were untreated, treated with heme (20 μM; H-control), heme-depleted, or heme-repleted after heme depletion, as detailed under *Materials and Methods*. A representative example of total eIF2α and eIF2αP Western immunoblotting analyses of these hepatocyte lysates (10 μg of protein) is shown at the top, with corresponding aliquots used for actin immunoblotting analyses as loading controls. Densitometric quantification of total hepatic eIF2α and eIF2αP content and corresponding statistically significant differences between mean ± S.D. of three individual experiments are shown at the bottom. Statistically significant differences in total eIF2α content were observed as indicated between the two values. Corresponding differences between eIF2αP content of the two mean ± S.D. values each marked with the same symbol were as follows: *, $p < 0.05$; **, $p < 0.05$.

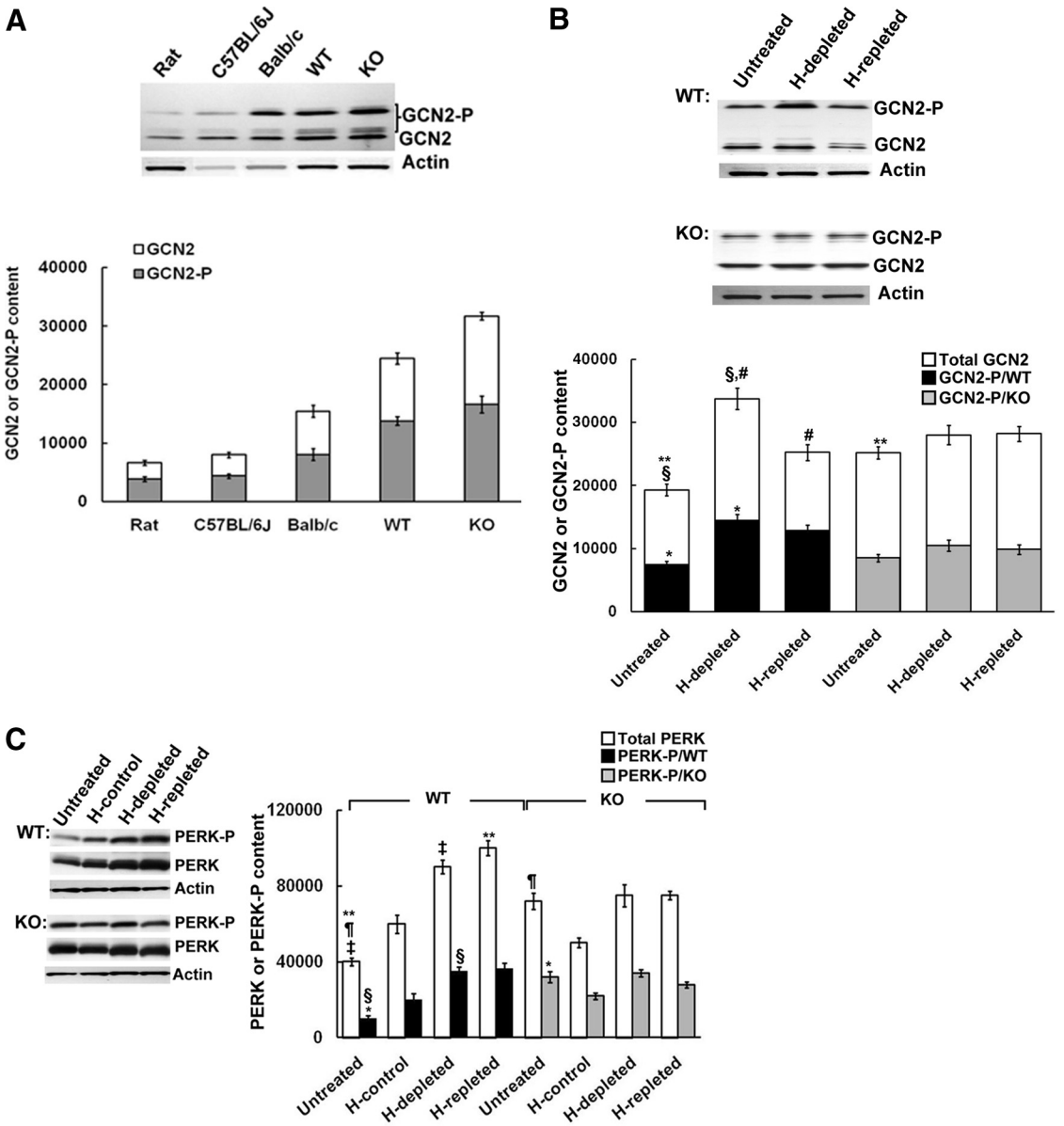

Fig. 5. Effects of acute hepatic heme depletion and repletion on hepatic content of GCN2 and PERK and their autophosphorylated species in cultured MGB wild-type [WT; HRI (+/+)] and HRI knockout [KO; HRI (−/−)] mouse hepatocyes. A, untreated rat or mouse (C57BL/6J, BALB/c, MGB WT, or KO) hepatocytes were cultured as detailed under *Materials and Methods*. A, a representative example of GCN2 and GCN2-P Western immunoblotting analyses of these hepatocyte lysates (50 μg of protein) are shown at the top, with corresponding smaller aliquots used for actin immunoblotting analyses as loading controls. Densitometric quantification of total hepatic GCN2 (GCN2 + GCN2-P) and autophosphorylated GCN2 (GCN2-P) content (mean ± S.D.) of three individual experiments is shown at the bottom. Statistically significant differences in hepatic GCN2 content were found between WT and KO lysates at $p < 0.001$, between WT and BALB/c at $p < 0.001$, or KO and BALB/c at $p < 0.001$, KO and rat at $p < 0.001$, and KO or WT and C57BL/6J at $p < 0.001$. Statistically significant differences in hepatic GCN2-P content were found between WT and KO lysates at $p < 0.05$, between WT and BALB/c at $p < 0.001$, between KO and BALB/c at $p < 0.001$, between KO and rat at $p < 0.001$, and between KO or WT and C57BL/6J at $p < 0.001$. B, WT or KO mouse hepatocyte cultures were untreated, heme (H)-depleted or heme-repleted after heme depletion, as detailed under *Materials and Methods*. A representative example of total GCN2 and GCN2-P Western immunoblotting analyses of these hepatocyte lysates (50 μg of protein) is shown at the top, with corresponding smaller aliquots used for actin immunoblotting analyses as loading controls. Densitometric quantification of total hepatic GCN2 (GCN2 + GCN2-P) and phosphorylated GCN2 (GCN2-P) content and corresponding statistically significant differences between mean ± S.D. of three individual experiments are shown at the bottom. Statistically significant differences were observed in the total hepatic GCN2 and GCN2-P content of untreated and H-depleted WT hepatocytes between the two mean ± S.D. values each marked with the same symbol as follows: §, $p < 0.001$; *, $p < 0.001$, respectively. Total hepatic GCN2 content of H-depleted WT cells was significantly different from that of H-repleted WT cells (#) at $p < 0.001$. Total hepatic GCN2 content of WT hepatocytes was significantly different from that of KO hepatocytes (**) at $p < 0.05$. No significant differences were found between any other values. C, WT or KO mouse hepatocyte cultures were untreated, treated with heme (20 μM; H-control), heme (H)-depleted, or heme-repleted after heme depletion, as detailed under *Materials and Methods*. PERK and PERK-P Western immunoblotting analyses of these hepatocyte lysates (100 μg of protein) are shown at the left, with corresponding smaller aliquots (10 μg of protein) of these same SDS-PAGE sample buffer-solubilized cell lysates used for actin immunoblotting analyses as loading controls. The densitometric quantification of the relative PERK-P content (solid bars) to the total PERK immunochemically detectable content (open bars) is shown at the right. Values represent mean ± S.D. of three separate experiments. Statistically significant differences in either PERK or PERK-P content between the two mean ± S.D. values each marked with the same symbol were as follows: *, $p < 0.001$; §, $p < 0.001$; ‡, $p < 0.001$; ¶, $p < 0.001$; and **, $p < 0.001$.

the basis of the protein concentration of each cell lysate, and the data were normalized on the basis of the immunoblots from lysates harvested at 0 h. In parallel, smaller aliquots (10 μg of protein) of the same SDS-PAGE sample buffer-solubilized cell lysates were subjected to actin immunoblotting analyses to verify that they matched the corresponding bicinchoninic acid assay-determined protein concentrations.

Ubiquitinated cellular protein was immunoblotted as described previously (Correia et al., 2005; Faouzi et al., 2007). CYP2B, CYP3A, TDO, eIF2α/eIF2αP, actin, Grp94, and Grp78/BiP were subjected to immunoblotting analyses as detailed elsewhere (Han et al., 2005b; Liao et al., 2007; Acharya et al., 2009). HRI protein was subjected to immunoblotting analyses with primary rabbit polyclonal antibodies against the corresponding recombinant rat hepatic HRI protein as described previously (Liao et al., 2007; Acharya et al., 2009). TER119 immunoblotting was performed to verify any potential erythroid contamination of the hepatocytes. Murine blood was used as the control both for TER119 and HRI derived from its <2% reticulocyte content.

Western immunoblotting analyses of PERK and PERK-P proteins was carried out with lysate protein (100 μg) as detailed elsewhere (Acharya et al., 2009) with rabbit polyclonal anti-PERK antibody and rabbit polyclonal anti-PERK-P (both from Santa Cruz Biotechnology, Santa Cruz, CA) as the primary antibody. BSA (5%) was used for blocking in the case of PERK-P. The authenticity of the PERK and PERK-P bands was confirmed as detailed previously (Acharya et al., 2009) by inclusion of lysates from hepatocytes treated with the PERK and ER-stress inducer thapsigargin, as well as lysates from SK-N-KH neuroblastoma-cells overexpressing recombinant PERK protein (Santa Cruz Biotechnology) as positive controls.

Western immunoblotting analyses of GCN2 and GCN2-P proteins were carried out with lysate protein (50 μg) as detailed previously (Acharya et al., 2009) with rabbit polyclonal anti-human GCN2 (Santa Cruz Biotechnology) as the primary antibody. The specificity of the commercial anti-GCN2 antibody was confirmed as detailed previously (Acharya et al., 2009) by parallel immunoblotting analyses with a monoclonal antibody raised against a mouse GCN2 carboxyl terminal domain and kindly provided by Prof. R. C. Wek. Lysates from commercially obtained HeLa cells overexpressing recombinant GCN2 protein (Santa Cruz Biotechnology) were also included as a positive control.

Densitometric Quantification. Direct quantification of the immunoblots was performed by ImageJ analyses.

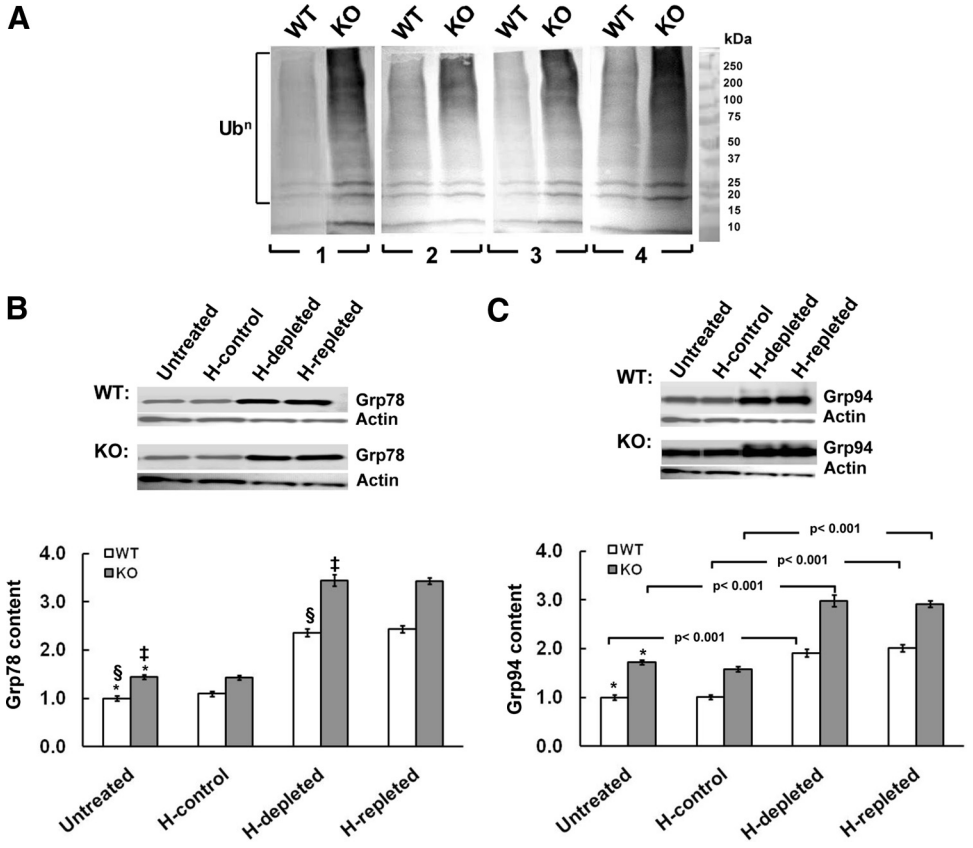

Fig. 6. Total hepatic protein ubiquitination and effects of acute hepatic heme depletion and repletion on hepatic content of ER-chaperones Grp78 and Grp94 in cultured MGB wild-type [WT; HRI (+/+)] and HRI knockout [KO; HRI (−/−)] mouse hepatocytes. A, untreated WT or KO mouse hepatocytes pooled from two mice each were cultured as detailed under *Materials and Methods* for each individual experiment. Hepatocyte lysates (50 μg of protein) from four individual experiments were prepared, and total hepatic protein ubiquitination was examined by Western immunoblotting analyses as described under *Materials and Methods*. B, WT or KO mouse hepatocyte cultures were untreated, treated with heme (20 μM; H-control), heme (H)-depleted, or heme-repleted after heme depletion, as in Fig. 5C. Aliquots (25 μg of protein) of these same SDS-PAGE sample buffer-solubilized cell lysates were used for Grp78 immunoblotting analyses and other aliquots (10 μg of protein) of these same SDS-PAGE sample buffer-solubilized cell lysates used for actin immunoblotting analyses as loading controls (Top). The densitometric quantification of the relative immunochemically detectable Grp78 content in KO (solid bars) to the WT (open bars) is shown below. Values represent mean ± S.D. of three separate experiments. Statistically significant differences in Grp78 content between the two mean ± S.D. values each marked with the same symbol were as follows: *, $p < 0.05$; §, $p < 0.001$; and ‡, $p < 0.001$. C, aliquots (25 μg of protein) of these same SDS-PAGE sample buffer-solubilized cell lysates were used for Grp94 immunoblotting analyses and other aliquots (10 μg of protein) used for actin immunoblotting analyses as loading controls (top). The densitometric quantification of the relative immunochemically detectable Grp94 content in KO (solid bars) to the WT (open bars) is shown below. Values represent mean ± S.D. of three separate experiments. Statistically significant differences in Grp94 content between the values were as indicated. The difference in basal Grp94 content of untreated WT and KO hepatocytes (*) was statistically significant at $p < 0.001$.

Quantitative Real-Time PCR Analyses. Total RNA was extracted with the RNAqueous-Micro kit (Ambion Inc., Austin, TX), treated with DNase to free it from DNA contamination using the Ambion DNA-free kit. This was followed by reverse transcription to cDNA by Moloney murine leukemia virus reverse transcriptase (Invitrogen) exactly as described previously (Han et al., 2005b). Universal PCR master mix and TaqMan primer-probe mixes were purchased from Applied Biosystems Inc. (Foster City, CA) for the detection of mouse mRNA sequences for CYP2B, Grp78, Grp94, and β-glucuronidase. The HRI primers were: CACTGCATGGATAGAGCACGTT (forward) and GGGCAGACGAATGTTAGGTC (reverse). The HRI-specific TaqMan probe was CGTGCTTCAGCCACAAG (Liao et al., 2007). The PCR reaction mixture (50 μl) was made as follows (final concentrations): 1× PCR master mix containing 1× TaqMan buffer, a 200 μM concentration of each dNTP, 1.5 units of AmpliTaq Gold DNA polymerase, 200 nM probes, 900 nM primers, nuclease-free water, and 10 ng of cDNA (from the reverse transcriptase reaction). PCR was performed in a MicroAmp ABI Prism 384-well clear optical reaction plate using the ABI Prism 7900 detector system. The initial denaturation cycle was at 95°C for 10 min followed by 40 cycles with denaturation at 95°C for 20 s and annealing/extension at 60°C for 1 min. The C_t (cycle number at which the fluorescent signal reaches the threshold level) value reflecting the expression of each gene was normalized to that of the endogenous control β-glucuronidase gene. Relative gene expression was calculated as $2^{-\Delta C_t}$, where ΔC_t is defined as C_t for gene of interest − C_t for β-glucuronidase. All values are expressed as percentage increase/decrease with respect to the RNA value in untreated hepatocytes.

Statistical Analyses. The Kolmogorov-Smirnov test was used to check whether the data followed normal distribution. Experiments were performed in triplicate. Data were compared by analysis of variance. p values <0.05 were considered statistically significant.

Results

HRI in Human, Rat, and Mouse Hepatocytes. To examine whether HRI is present in human and mouse hepatocytes, we carried out parallel immunoblotting analyses with freshly isolated and Percoll-sedimentation gradient-purified parenchymal cells (hepatocytes) from human, rat, and C57BL/6J, BALB/c, MGB (C57BL/6-S129) HRI wild-type [WT; HRI(+/+)], and MGB HRI knockout [KO; HRI(−/−)] mouse livers (Fig. 1A), as well as corresponding cultured human, mouse, and size-elutriated rat hepatocytes (Fig. 1B), along with reticulocyte HRI in mouse blood as positive controls (Fig. 1). Our findings revealed that HRI protein constitutively exists as the native nonphosphorylated 76-kDa species and/or the autoactivated/autophosphorylated 92-kDa species in many of the cells examined, although the relative abundance of each HRI species tends to vary. The predictable exception was the MGB HRI-KO mouse hepatocyte, in which both HRI species were absent consistent with its genetic knockout and nullizygosity.

It is noteworthy that the hyperphosphorylated 92-kDa HRI was the species predominantly detected in the HRI(+/+)-WT mouse hepatocytes (Fig. 1). A relatively large fraction of the BALB/c mouse hepatic HRI was also constitutively hyperphosphorylated (92-kDa species), and this was slightly enhanced upon culturing (Fig. 1B), in contrast to that of its C57BL/6J mouse counterpart (Fig. 1A). However, some HRI hyperphosphorylation was also detected upon culture of C57BL/6J mouse hepatocytes (Fig. 1A). Parallel immunoblotting analyses with anti-TER119, a monoclonal antibody that is a sensitive and specific late erythroid cell lineage marker (Zhang et al., 2003), readily recognized erythroid Ly-76 antigen associated with glycophorin A in red blood cells (10 or 20 μg of protein) but in none of the hepatocyte preparations, even upon loading of 100 μg of lysate protein (Fig. 1). These findings thus conclusively excluded any erythroid contamination of the hepatocytes, thereby revealing that the HRI detected was intrinsically hepatic in origin.

Furthermore, the identity of the 92-kDa HRI species as autophosphorylated HRI was verified by in vitro treatment of BALB/c and C57BL/6J mouse hepatocyte lysates with and without calf intestinal alkaline phosphatase at 37°C for 1 h (Lu et al., 2001; Fig. 1C). This treatment duly dephosphorylated the hepatic HRI 92-kDa species, reverting it to its unphosphorylated 76-kDa species (Fig. 1C). The functional import of the constitutive hepatic HRI autophosphorylation was assessed by analyses of the relative basal hepatic eIF2αP and eIF2α content of the corresponding lysates (Fig. 1D). These findings revealed that with the exception of HRI(−/−) lysates (for reasons detailed below), the relative hepatic eIF2αP content of the other lysates mirrored the corresponding extent of their constitutively autophosphorylated 92-kDa HRI species (Fig. 1, A and B).

Treatment of cultured rat hepatocytes with various P450 inducers such as PB, Dex, carbamazepine, rifampin, and

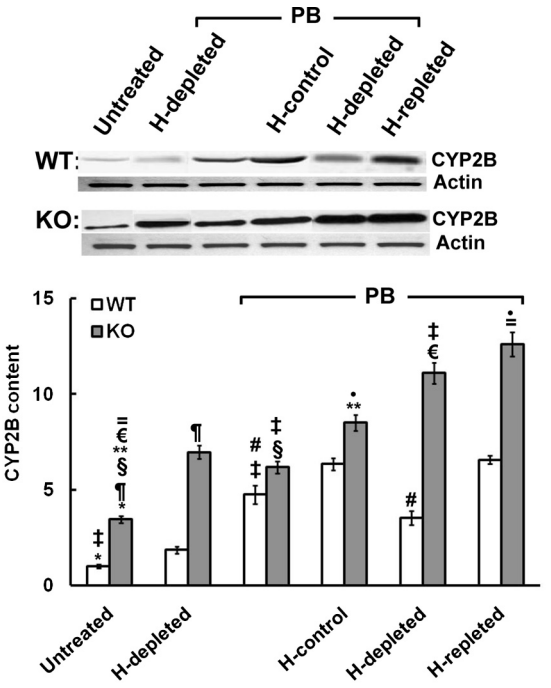

Fig. 7. Effects of acute hepatic heme depletion and repletion on PB-mediated CYP2B induction in cultured MGB wild-type [WT; HRI (+/+)] and HRI knockout [KO; HRI (−/−)] mouse hepatocytes. WT or KO mouse hepatocyte cultures were untreated or heme (H)-depleted (first two lanes), or pretreated with PB (next four lanes): alone (lane 3), with heme (H-control; lane 4), heme depletion (H-depleted; lane 5), or heme repletion after heme depletion (H-repleted; lane 6), as detailed under *Materials and Methods*. A representative example of CYP2B Western immunoblotting analyses of these hepatocyte lysates (30 μg of protein) is shown at the top, with corresponding aliquots used for actin immunoblotting analyses as loading controls. Densitometric quantification of hepatic CYP2B content from three individual experiments is shown at the bottom. Statistical analyses revealed significant differences in hepatic CYP2B content between the two mean ± S.D. values each marked with the same symbol as follows: ∗, $p < 0.001$; §, $p < 0.001$; ‡, $p < 0.001$; ¶, $p < 0.001$; €, $p < 0.001$; #, $p < 0.001$; =, $p < 0.001$; and ∗∗, $p < 0.001$. No statistically significant differences were observed between PB-pretreated/H-control and PB/H-repleted WT lysates.

barbituric acid revealed significant induction of total hepatic HRI content and autoactivation (HRI-P) with all inducers except carbamazepine (Fig. 1E).

Activation of Hepatic HRI in Acute Heme-Depleted C57BL/6J Mouse Hepatocytes: Reversal by Heme. The available genetic HRI(−/−) KO mouse (Han et al., 2001; Lu et al., 2001) in principle should be an appropriate model to probe the physiological role of hepatic HRI in general and the heme-mediated regulation of CYP2B induction in particular. However, before embarking on these studies, it was important to verify that our findings in rat hepatocytes extended to the mouse hepatocytes. We therefore examined the heme-sensitivity of the hepatic HRI autoactivation and its corresponding eIF2α kinase activity in hepatocytes from C57BL/6J mice that were untreated, acutely depleted of heme (H-depleted), or repleted with heme after acute heme depletion (H-repleted) (Fig. 2A). In its basal cultured state, the HRI protein existed largely as the 76-kDa species in C57BL/6J mouse hepatocytes. It is noteworthy that acute heme depletion led not only to an increase in the total hepatic HRI content but also to its functional activation (Fig. 2A). Indeed, the marked increase in the 92-kDa HRI species (HRI-P) after acute hepatic heme depletion revealed that relative to its basal state, the HRI protein in C57BL/6J mouse hepatocytes was almost fully autophosphorylated, and this was largely inhibited by heme repletion (Fig. 2A). Consistent with this marked HRI activation via autophosphorylation, its eIF2α kinase activity was also markedly increased after hepatic heme depletion as reflected by the relatively increased eIF2αP fraction of the total hepatic eIF2α content (Fig. 2B). As expected from its characteristic heme sensitivity, this activation was also abrogated by heme repletion (*Fig. 2B*). Accordingly, in common with the findings of PB-inducible CYP2B1/2B2 in heme-depleted rat hepatocytes (Han et al., 2005b), this marked HRI activation also greatly impaired the PB-mediated induction of mouse hepatic CYP2B in heme-depleted mouse hepatocytes (Fig. 2C). This impairment was similarly reversed by heme repletion (Fig. 2C). Moreover, consistent with the global hepatic protein translational shutoff after HRI activation, a similar parallel impairment of hepatic CYP3A, another PB-inducible ER-bound P450 (see below) and hepatic cytosolic TDO (Fig.

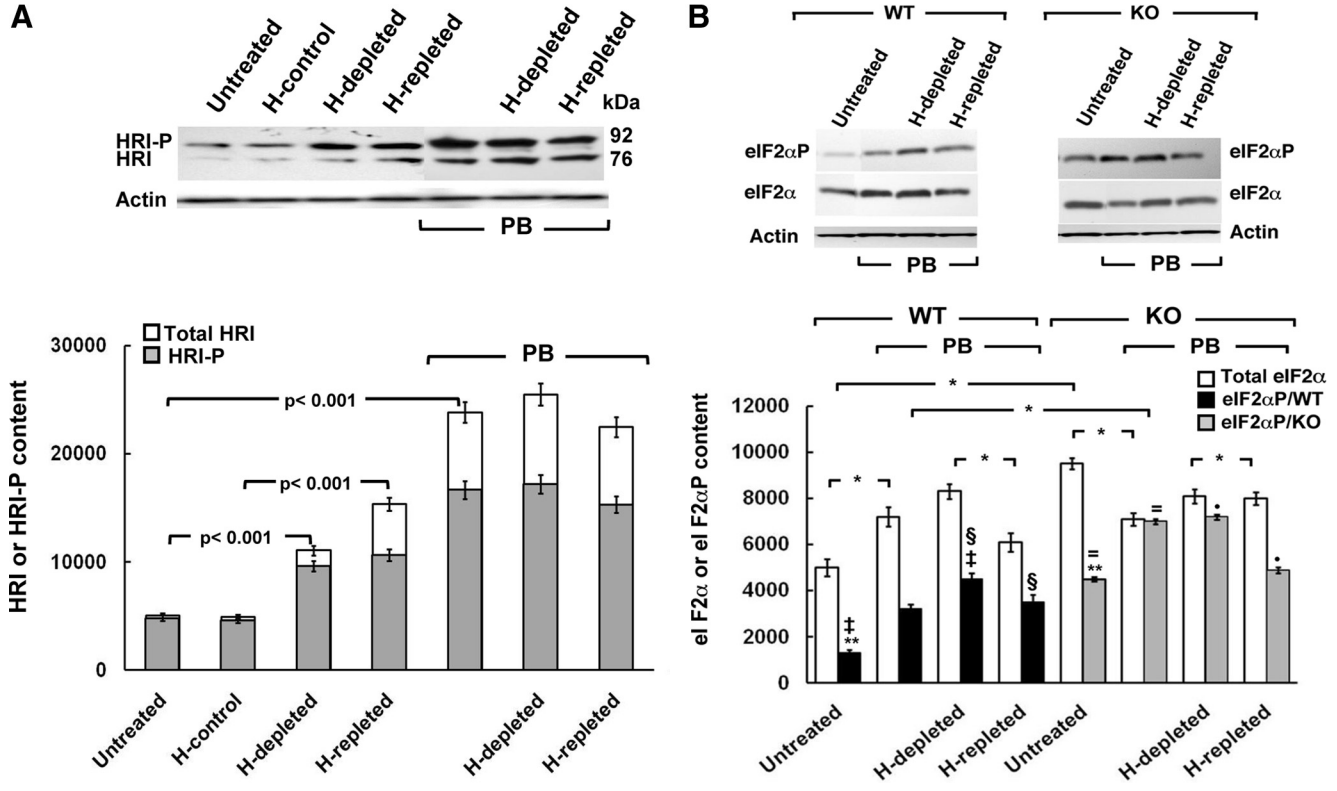

Fig. 8. Effects of acute hepatic heme depletion and repletion on hepatic HRI content and autophosphorylation, and eIF2α kinase activity in cultured MGB wild-type [WT; HRI (+/+)] mouse hepatocytes with and without PB pretreatment. A, WT mouse hepatocyte cultures were untreated, treated with heme (H-control), heme-depleted (H-depleted), or heme-repleted after heme depletion (H-repleted) (first four lanes), or pretreated with PB (next three lanes) alone (lane 5), heme-depleted (H-depleted; lane 6), or heme-repleted after heme depletion (H-repleted ; lane 7), as detailed under *Materials and Methods*. A representative example of HRI and HRI-P Western immunoblotting analyses of these hepatocyte lysates (100 μg of protein) is shown at the top, with corresponding smaller aliquots (10 μg of protein) of these same SDS-PAGE sample buffer-solubilized cell lysates used for actin immunoblotting analyses as loading controls. Densitometric quantification of total hepatic HRI and HRI-P content from three individual experiments is shown at the bottom. Statistical analyses revealed significant differences in both hepatic HRI and HRI-P content between untreated and PB-pretreated at $p < 0.001$, and between PB/H-repleted and PB/H-depleted at $p < 0.05$. No statistically significant differences were observed between PB/H-depleted and PB-pretreated or between PB-pretreated and PB/H-repleted WT lysates. B, WT or KO mouse hepatocyte cultures were untreated or pretreated with PB alone (lane 2) and then either heme-depleted (lane 3) or heme-repleted after heme depletion (lane 4), as detailed under *Materials and Methods*. A representative example of total eIF2α and eIF2αP Western immunoblotting analyses of these hepatocyte lysates (10 μg of protein) is shown at the top with corresponding aliquots used for actin immunoblotting analyses as loading controls. Densitometric quantification of total hepatic eIF2α and eIF2αP content, and corresponding statistically significant differences between mean ± S.D. of 3 individual experiments are shown at the bottom. Statistically significant differences in eIF2α or eIF2αP content were observed between the two mean ± S.D. values each marked with the same symbol as follows: *, $p < 0.001$; §, $p < 0.001$; ‡, $p < 0.001$; =, $p < 0.001$; ●, $p < 0.001$; and **, $p < 0.001$.

2D) was observed in heme-depleted hepatocytes. Both these effects were also similarly reversed by heme repletion, in common with the CYP2B1/2B2 findings (Fig. 2C). These collective observations are entirely consistent with the characteristic heme-sensitivity of hepatic HRI and its critical heme-regulated translational control of hepatic protein synthesis,

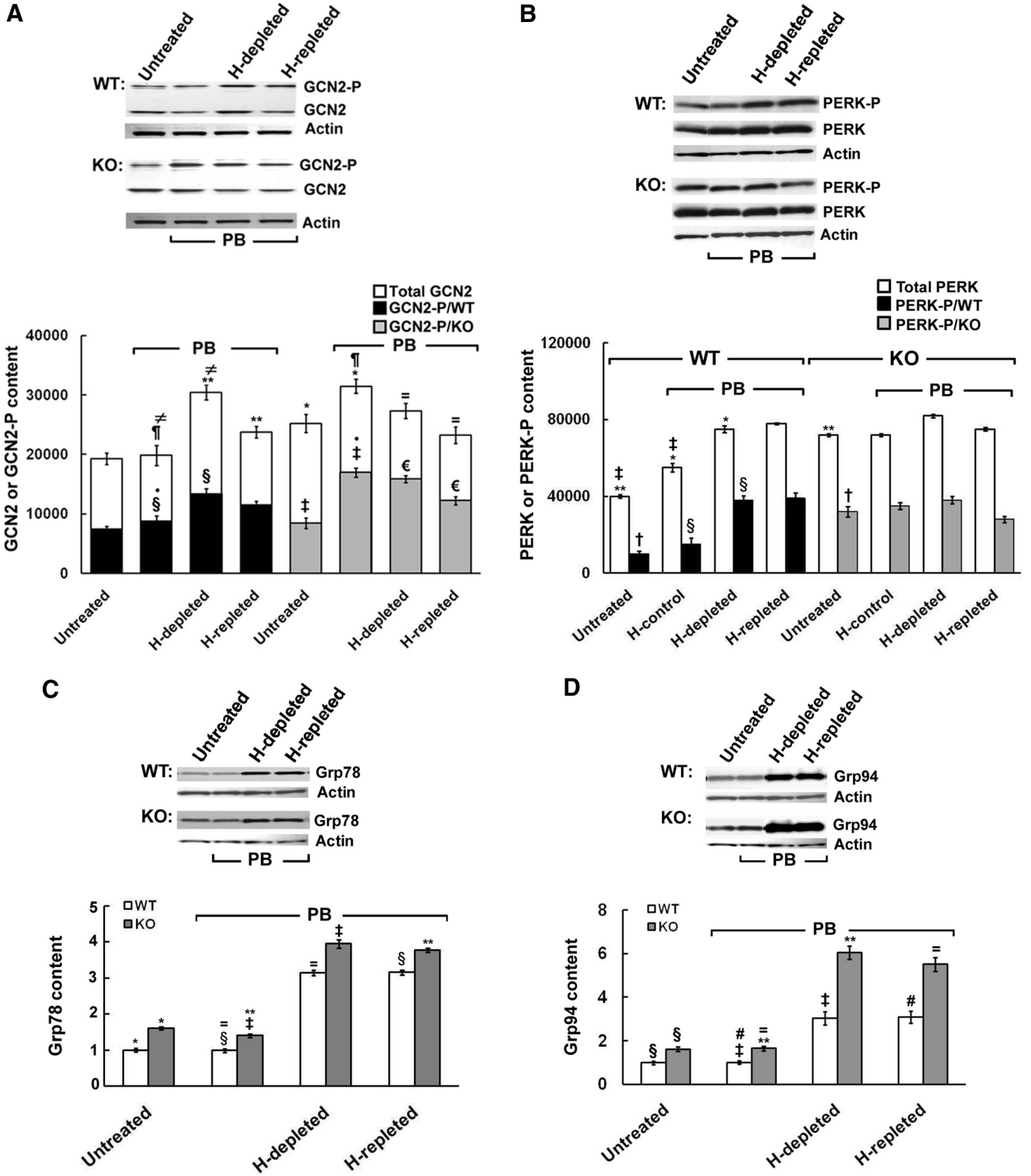

Fig. 9. Effects of acute hepatic heme depletion and repletion on the hepatic content of GCN2 and PERK and their autophosphorylated species, Grp78 and Grp94 content in cultured MGB wild-type [WT; HRI (+/+)] and HRI knockout [KO; HRI (−/−)] mouse hepatocytes with and without PB-pretreatment. A, WT or KO mouse hepatocyte cultures were untreated or pretreated with PB alone (lane 2) and then either heme (H)-depleted (lane 3), or heme-repleted after heme depletion (lane 4), as detailed under *Materials and Methods*. A representative example of total GCN2 and GCN2-P Western immunoblotting analyses of these hepatocyte lysates (50 μg of protein) is shown with corresponding smaller aliquots (10 μg of protein) of these same SDS-PAGE sample buffer-solubilized cell lysates used for actin immunoblotting analyses as loading controls at the top.

as documented previously (Han et al., 2005b; Liao et al., 2007).

The specific inverse relationship between hepatic heme status and HRI eIF2α kinase function was further confirmed by examination of two other plausible hepatic eIF2α kinase candidates: GCN2 and PERK.[1] Hepatic heme depletion and repletion failed to similarly affect either of these hepatic eIF2α kinases, consistent with their known lack of heme-recognition motifs and heme responsiveness (Fig. 3, A and B). Together, these findings not only confirm the reciprocal relationship of hepatic HRI function to the hepatic heme availability in the mouse but also reveal that hepatic HRI functions similarly in the C57BL/6J mouse and the Sprague-Dawley rat (Han et al., 2005b; Liao et al., 2007).

Physiological Role of Hepatic HRI. In an attempt to probe the cellular role of hepatic HRI, we examined eIF2α kinase activity in MGB WT [HRI(+/+)] and MGB KO [HRI(−/−)] mouse hepatocytes (Fig. 4). Intriguingly, we found that despite the absence of any hepatic HRI protein (Fig. 1), the basal eIF2α kinase activity in untreated HRI(−/−) mouse hepatocytes was appreciably elevated over the corresponding HRI(+/+) mouse hepatocytes (Fig. 4). Alterations of hepatic heme pool size had little effect on the content of either total eIF2α or phosphorylated eIF2α (eIF2αP) in these HRI(−/−) mouse hepatocytes. By contrast, parallel manipulations of the hepatic heme pool increased the content of total eIF2α as well as that of eIF2αP in HRI(+/+) mouse hepatocytes (Fig. 4A). In these WT cells, both heme depletion and heme repletion contributed to further significant increases in total eIF2α content as well as enhancement of eIF2α kinase activity over basal levels (Fig. 4A). This is in striking contrast to our findings in wild-type C57BL/6J mouse (Fig. 2B) and Sprague-Dawley rat hepatocytes (Han et al., 2005b; Liao et al., 2007). Thus, although HRI exists in these HRI(+/+) hepatocytes, it is predominantly in its hyperphosphorylated 92-kDa form, which apparently is largely refractory to cellular heme fluctuations. To verify whether this was indeed the case, we examined BALB/c mouse hepatocytes that also exhibit constitutively hyperphosphorylated 92-kDa HRI as the predominant species (Fig. 1). We found these hepatocytes to be similarly unresponsive to heme depletion or repletion, thereby reiterating the findings in HRI(+/+) hepatocytes (Fig. 4B). Together, these findings reveal that the hyperphosphorylated 92-kDa HRI species in HRI(+/+) or BALB/c mouse hepatocytes lacks the heme-responsiveness of its counterparts in rat or C57BL/6J mouse hepatocytes.

Basal ER-Stress Induction after Genetic HRI Knockdown. To identify the eIF2α kinase(s) responsible for the significantly elevated eIF2αP in MGB HRI(−/−) mouse hepatocytes (Fig. 4), we examined the relative autoactivation/autophosphorylation of the two other plausible hepatic eIF2α kinase candidates, GCN2 and PERK. The basal levels of both total GCN2 and its autoactivated/autophosphorylated GCN2-P species were significantly elevated in MGB KO/HRI(−/−) mouse hepatocytes over the corresponding MGB WT/HRI(+/+) hepatocytes (Fig. 5A). However, these GCN2 and GCN2-P values in both HRI(−/−) and HRI(+/+) mouse hepatocytes were considerably higher than the corresponding basal values in the untreated rat, C57BL/6J, or BALB/c mouse hepatocytes (Fig. 5A). Hepatic heme depletion and subsequent repletion enhanced the total GCN2 content and the relative GCN2-P fraction in HRI(+/+) but not in HRI(−/−) mouse hepatocytes (Fig. 5B). The basal content of PERK and that of its autoactivated/autophosphorylated species (PERK-P) were significantly increased 2- and 3.5-fold, respectively, in HRI(−/−) relative to those in HRI(+/+) mouse hepatocytes (Fig. 5C). Manipulations of the hepatic heme pool had little further effect on total PERK or PERK-P content in HRI(−/−) mouse hepatocytes (Fig. 5C). By contrast, consistent with the significant enhancement of eIF2α kinase activity over basal levels, hepatic heme manipulations also significantly increased both total PERK and PERK-P content in HRI(+/+) mouse hepatocytes. This is, once again, in marked contrast to the PERK response of wild-type C56BL/6J mouse and rat hepatocytes to similar hepatic heme pool alterations (Han et al., 2005b; Liao et al., 2007; Fig. 3).

The significantly elevated basal PERK-P content and consequently significantly elevated eIF2αP in MGB HRI(−/−) mouse hepatocytes relative to the corresponding values in MGB HRI(+/+) mouse hepatocytes were associated with enhanced hepatic protein ubiquitination, a reflection of extant ER-stress (Fig. 6A). However, despite this PERK activation, the basal levels of the ER chaperones Grp78 (BiP) and Grp94 were only slightly, albeit

[1] Double-stranded RNA-activated PKR is usually induced by viral inducers or class 1 interferons (which were not specifically included in the cell culture) and was therefore not examined.

Corresponding densitometric quantification of total hepatic GCN2 and GCN2-P content (mean ± S.D.) of three individual experiments is shown at the bottom. Statistically significant differences were observed in total hepatic GCN2 and GCN2-P content of untreated WT and KO hepatocytes between the two mean ± S.D. values each marked with the same symbol as follows: *, $p < 0.001$; §, $p < 0.001$; ‡, $p < 0.001$; ¶, $p < 0.001$; €, $p < 0.001$; =, $p < 0.001$; ●, $p < 0.001$; ≠, $p < 0.001$; and **, $p < 0.001$. B, aliquots of the same SDS-PAGE sample buffer-solubilized cell lysates (100 μg of protein) used in A were subjected to total PERK and PERK-P Western immunoblotting analyses with corresponding smaller aliquots (10 μg of protein) used for actin immunoblotting analyses as loading controls. A representative example of these immunoblots is shown at the top. Corresponding densitometric quantification of total hepatic PERK and PERK-P content (mean ± S.D.) of three individual experiments is shown at the bottom. Statistically significant differences were observed between total hepatic PERK or PERK-P content of untreated WT and KO hepatocytes between the two mean ± S.D. values each marked with the same symbol as follows: *, $p < 0.001$; §, $p < 0.001$; ‡, $p < 0.001$; †, $p < 0.001$; and **, $p < 0.001$. C, aliquots of these SDS-PAGE sample buffer-solubilized cell lysates (25 μg of protein) used in A were subjected to Grp78 Western immunoblotting analyses with corresponding aliquots (10 μg of protein) used for actin immunoblotting analyses as loading controls. A representative example of these immunoblots is shown at the top. Corresponding densitometric quantification of total hepatic Grp78 content (mean ± S.D.) of three individual experiments is shown at the bottom. Statistically significant differences were observed between Grp78 content of untreated WT and KO hepatocytes between the two mean ± S.D. values each marked with the same symbol as follows: *, $p < 0.001$; §, $p < 0.001$; ‡, $p < 0.001$; =, $p < 0.001$; and **, $p < 0.001$. D, aliquots of these SDS-PAGE sample buffer-solubilized cell lysates (25 μg of protein) used in A were subjected to Grp94 Western immunoblotting analyses with corresponding aliquots (10 μg of protein) used for actin immunoblotting analyses as loading controls. A representative example of these immunoblots is shown at the top. Corresponding densitometric quantification of total hepatic Grp94 content (mean ± S.D.) of three individual experiments is shown at the bottom. Statistically significant differences were observed between the two mean ± S.D. values each marked with the same symbol as follows: **, $p < 0.001$; §, $p < 0.05$; ‡, $p < 0.001$; =, $p < 0.001$; and #, $p < 0.001$. No statistically significant differences were observed with PB/H-depleted and PB/H-repleted for either WT or KO cells.

significantly elevated in HRI(−/−) mouse hepatocytes (Fig. 6, B and C). Heme depletion/repletion further increased hepatic Grp78 and Grp94 content in both HRI(+/+) and HRI(−/−) mouse hepatocytes, although this increase was more pronounced in the latter (Fig. 6, B and C).

Role of HRI in CYP2B Induction. We have shown previously that heme regulates PB-mediated CYP2B1/2 induction translationally rather than transcriptionally in the rat liver possibly by controlling hepatic HRI activity (Han et al., 2005b). This heme-regulated translational control of HRI can also be documented in the PB induction of hepatic CYP2B in C57BL/6J mouse hepatocytes (Fig. 2C). Thus, as proof of principle, genetic ablation of HRI in HRI(−/−) mouse hepatocytes would be expected to abolish this response to acute hepatic heme depletion by eliminating the translational initiation control exerted through HRI autoactivation. Indeed, we found that acute hepatic heme depletion of MGB HRI(−/−) mouse hepatocytes had no effect on their PB-mediated CYP2B induction (Fig. 7), in contrast to its impairment in wild-type MGB HRI(+/+) mouse hepatocytes (Fig. 7) and wild-type C57BL/6J cells (Fig. 2C). Thus, genetic deletion of hepatic HRI rendered PB-mediated CYP2B protein induction independent of hepatic heme status and/or fluctuations (Fig. 7). Accordingly, despite the significant basal activation of GCN2 and PERK eIF2α kinases in the untreated HRI(−/−) hepatocytes, their basal CYP2B levels were significantly higher than those in HRI(+/+) mouse hepatocytes and were further elevated on heme depletion (Fig. 7). It is noteworthy that PB-mediated CYP2B protein induction progressed supranormally even in the absence of heme (Fig. 7). Furthermore, PB-inducible CYP2B protein content of HRI(−/−) hepatocytes, albeit slightly higher in heme-repleted versus heme-depleted hepatocytes, was consistently higher than that observed in correspondingly treated wild-type HRI(+/+) hepatocytes (Fig. 7). However, unlike the findings in untreated (non–PB-treated) HRI(+/+) mouse hepatocytes, in which HRI was almost fully autophosphorylated in the basal state and thus refractory to hepatic heme pool alterations (Fig. 4), PB treatment apparently restored some of the heme-sensitivity of HRI in MGB HRI(+/+) mouse hepatocytes (Fig. 8A). This is reflected by the eIF2α kinase activation by heme depletion and its reversal by heme repletion in PB-treated HRI(+/+) hepatocytes (Fig. 8B). Such findings, however, are normal in C57BL/6J mouse hepatocytes (Fig. 2A) and rat hepatocytes (Han et al., 2005b; Liao et al., 2007). We also find it remarkable that PB treatment of MGB mouse HRI(+/+) hepatocytes led to an overall increase in total hepatic HRI content, a significant fraction of which remained in its native nonactivated/autophosphorylated state and thus susceptible to heme-inhibition (Fig. 8A).

Effects of PB Treatment on PERK and GCN2 Content and Autoactivation and ER Chaperone Induction in MGB HRI(+/+) and HRI(−/−) Hepatocytes. After treatment with PB alone, no major differences were observed in hepatic GCN2 content in HRI(+/+) mouse hepatocytes relative to corresponding untreated HRI(+/+) hepatocytes (Fig. 9A). In these PB-treated HRI(+/+) cells, heme depletion similarly resulted in a significant increase in total hepatic GCN2 content and its autophosphorylated species (Fig. 9A) just as in the corresponding untreated cells (Fig. 5B). This increase in total GCN2 content and autophosphorylation upon heme depletion was reversed on heme repletion (Fig. 9A). On the other hand, a larger fraction of hepatic GCN2 seemed to be in the autoactivated/autophosphorylated state, irrespective of hepatic heme pool alterations after PB treatment of HRI(−/−) mouse hepatocytes (Fig. 9A).

Treatment of MGB HRI(+/+) mouse hepatocytes with PB alone had no significant effect on PERK autophosphorylation and led to only a minor, albeit significant, increase in total PERK content relative to untreated HRI(+/+) mouse hepatocytes (Fig. 9B). Both parameters, however, were significantly enhanced upon hepatic heme pool alterations in PB-treated HRI(+/+) cells (Fig. 9B) just as in the untreated HRI(+/+) mouse hepatocytes (Fig. 5C). PB-pretreatment or hepatic heme alterations had no significant further effect on total PERK or PERK-P content of HRI(−/−) mouse hepatocytes over basal levels (Fig. 9B). Modulation of the hepatic heme pool significantly increased hepatic Grp78 content in both PB-treated HRI(+/+) and HRI(−/−) mouse hepatocytes (Fig. 9C), and this seemed to be more pronounced in HRI(−/−) over the HRI(+/+) mouse hepatocytes (Fig. 9C). Similar effects were also observed with hepatic Grp94 content, although the differences were much more pronounced in the HRI(−/−) over the HRI(+/+)mouse hepatocytes (Fig. 9D).

Verification of the Physiological Role of HRI in Pure C57BL/6J-Background Mouse HRI(−/−) Hepatocytes. Because of the striking differences between MGB HRI(+/+) and pure background C57BL/6J HRI(+/+) mouse hepatocytes, it was important to exclude strain-associated responses. The availability of a few (n = 5) pure-background C57BL/6J HRI(−/−) mice enabled us to verify and extend our most important findings in MGB HRI(−/−) hepatocytes (Fig. 10). Using C57BL/6J WT HRI(+/+) mice as parallel controls (Fig. 2, C and D, and 10A), we found that PB induction of both CYP2B and CYP3A was independent of hepatic heme status and proceeded undeterred in the C57BL/6J HRI(−/−) mouse hepatocytes, unlike that in C57BL/6J HRI(+/+) mouse hepatocytes (Fig. 10A). This finding was very similar to that in the MGB HRI(−/−) mouse hepatocytes (Fig. 7). qRT-PCR analyses of total RNA from C57BL/6J WT and HRI(−/−) hepatocytes with a CYP2B10-specific Taqman probe revealed that in both C57BL/6J WT and HRI(−/−) hepatocytes, CYP2B mRNA was indeed PB-inducible but was unaffected by concomitant hepatic heme depletion or repletion (Fig. 10B), consistent with previous findings (Srivastava et al., 1989; Sinclair et al., 1990; Jover et al., 2000; Han et al., 2005b). However, irrespective of hepatic heme depletion or repletion, CYP2B mRNA levels were slightly albeit significantly higher in the HRI(−/−) hepatocytes than in the corresponding WT hepatocytes (Fig. 10B).[2] This relative increase was further magnified after PB treatment (Fig. 10B).

Pulse-chase analyses with [^{35}S]Met/Cys coupled with CYP2B immunoprecipitation analyses of lysates from PB-treated C57BL/6J WT hepatocytes after heme depletion or repletion and subsequent SDS-PAGE/PhosphorImager analyses of CYP2B immunoprecipitates revealed the HRI-medi-

[2] It is entirely plausible that the slightly albeit significantly higher CYP2B mRNA in the HRI(−/−) hepatocytes than in the corresponding WT hepatocytes results from the ER stress-inducible hepatic ATF5 and ATF4 transcription factors that are abundant and reportedly cooperate with the constitutive androstane receptor-mediated CYP2B6 mRNA induction in HepG2 cells (Pascual et al., 2008).

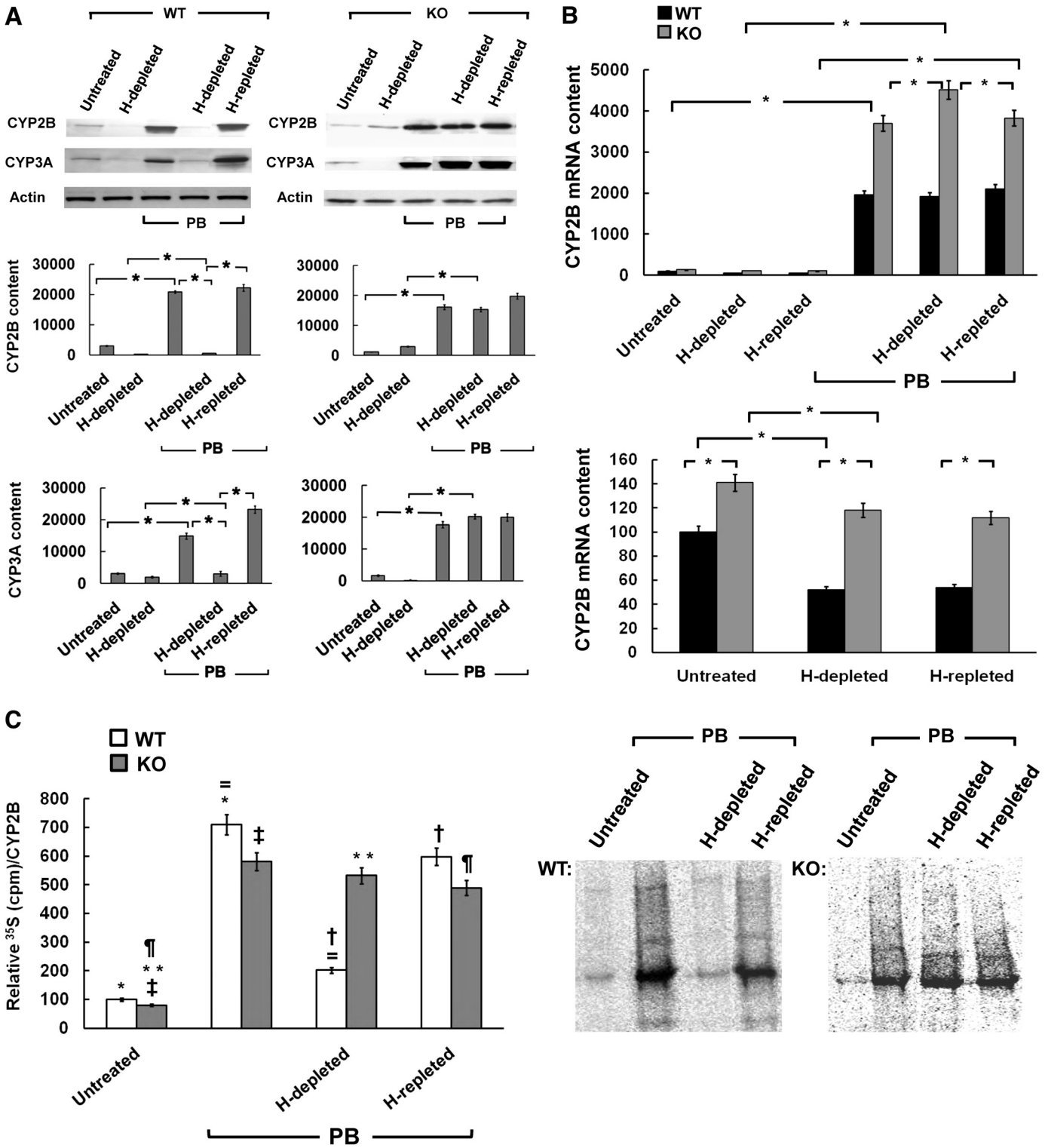

Fig. 10. Effects of heme depletion or repletion on PB-mediated induction of hepatic CYP2B and CYP3A in C57BL/6J HRI (−/−; KO) hepatocytes and corresponding HRI (+/+; WT) controls. A, treatments were carried out exactly as detailed under *Materials and Methods*. Values are mean ± S.D. of three separate experiments. Statistically significant differences between two individual values are as shown by the ∗ ($p < 0.001$). B, qRT-PCR analyses of total RNA from cultured hepatocytes treated as in A are shown at the top. Values are mean ± S.D. of three separate experiments. Statistically significant differences between the two individual values are as shown by the ∗ ($p < 0.001$). A magnified graph of the CYP2B mRNA values in untreated hepatocytes (non–PB-treated) included at the top are shown at the bottom. C, pulse-chase and CYP2B immunoprecipitation analyses of untreated and PB-pretreated hepatocytes are shown at the bottom. The relative [^{35}S]Met/Cys incorporated into equivalent aliquots of CYP2B immunoprecipitates monitored by scintillation counting is shown on the left. Statistically significant differences were observed between the two mean ± S.D. values each marked with the same symbol at $p < 0.001$. The corresponding Typhoon 9400 analyses of corresponding CYP2B immunoprecipitate aliquots subjected to SDS-PAGE are shown on the right.

ated translational arrest of CYP2B synthesis that was relieved upon heme repletion (Fig. 10C), consistent with our findings in rat hepatocytes (Han et al., 2005b). Genetic HRI deletion effectively abolished this translational arrest of CYP2B synthesis in HRI(−/−) hepatocytes, rendering PB-induced CYP2B translation refractory to hepatic heme status (Fig. 10C). qRT-PCR analyses of total RNA from untreated C57BL/6J WT and HRI(−/−) hepatocytes with a HRI-specific TaqMan probe verified virtual genetic deletion of hepatic HRI[3] (Fig. 11). Corresponding qRT-PCR analyses of total RNA from PB-treated C57BL/6J WT and HRI(−/−) hepatocytes indicated that PB indeed induced hepatic HRI mRNA content in the WT but not HRI(−/−) hepatocytes (Fig. 11), consistent with similar observations of PB-mediated HRI protein induction in MGB WT hepatocytes (Fig. 8A). Collectively these findings in C57BL/6J HRI(−/−) hepatocytes are essentially similar to those obtained in MGB HRI(−/−) hepatocytes and are consistent with HRI-mediated translational control of CYP2B and CYP3A induction by PB.

To determine whether genetic HRI deletion also similarly enhanced basal ER-stress in C57BL/6J HRI(−/−) hepatocytes, the relative content of eIF2α and eIF2αP was monitored in lysates from untreated and PB-treated C57BL/6J WT and HRI(−/−) hepatocytes (Fig. 12). Untreated C57BL/6J HRI(−/−) hepatocytes exhibited higher basal hepatic eIF2α and eIF2αP content than the corresponding WT controls (Fig. 12A), with a profile very similar to that observed in untreated MGB HRI(−/−) hepatocytes (Fig. 4). Also similar was that hepatic heme depletion or repletion had very little additional effect on these levels (Fig. 12A). PB treatment of C57BL/6J HRI(−/−) hepatocytes further increased basal hepatic eIF2α and eIF2αP content over corresponding WT control levels (Fig. 12B), very similarly to that observed in MGB HRI(−/−) hepatocytes (Fig. 8B). Once again, hepatic heme depletion or repletion had very little additional effect on these levels (Fig. 12B), as is the case in PB-treated MGB HRI(−/−) hepatocytes (Fig. 8B).

In addition, qRT-PCR analyses with mouse Grp78- and Grp94-specific TaqMan probes of total RNA from untreated or PB-treated C57BL/6J WT and HRI(−/−) hepatocytes along with total RNA from C57BL/6J WT hepatocytes treated with the ER-stress inducer thapsigargin (10 μM) as a positive control, indicated a relatively weak, albeit statistically significant increase in basal Grp78 and Grp94 mRNA content in C57BL/6J HRI(−/−) hepatocytes over corresponding WT control cells (Fig. 12, C and D). PB treatment further increased these responses in both C57BL/6J WT and HRI(−/−) hepatocytes (Fig. 12, C and D). Collectively, these findings reveal essentially similar responses to heme depletion or repletion in either the untreated or PB-treated state of HRI(−/−) hepatocytes from the C57BL/6J mice to those from MGB mice, thereby validating the conclusions drawn from the findings in HRI(−/−) hepatocytes from MGB mice.

Discussion

Our findings reveal that in common with the rat hepatocytes, human and mouse hepatocytes also contain significant levels of HRI eIF2α kinase. However, although the hepatic HRI levels are apparently lower than those of erythroid cells on per mg protein basis,[4] this may be due to the HRI protein dilution by the overall highly diverse composition and more abundant protein content of the larger hepatocyte. This consideration, along with the relatively large size of the intact liver, implies physiologically significant hepatic HRI capacity.

By every criteria examined, the C57BL/6J mouse hepatic HRI behaves as a bona fide HRI: it is autoactivated via autophosphorylation by acute hepatic heme depletion (Fig. 2A), just like its rat counterpart (Han et al., 2005b; Liao et al., 2007), and its eIF2α kinase activity is similarly inhibited by heme (Fig. 2B). Furthermore, its activation after acute hepatic heme depletion similarly impairs PB-mediated CYP2B induction that is reversed by heme repletion (Figs. 2C and 10, A and C). Genetic HRI knockout in mouse hepatocytes abolished this particular CYP2B response to heme depletion, and the CYP2B protein continued to accumulate to supranormal levels, irrespective of the hepatic heme pool status (Figs. 7 and 10A). However, it remains to be determined whether this CYP2B protein synthesized in heme-depleted HRI(−/−) hepatocytes is a functionally active P450 hemoprotein. Nevertheless, taken together, these findings document that HRI is a protagonist in the heme-mediated translational control of hepatic CYP2B induction, and its genetic ablation derails this control (Fig. 13). Furthermore, the very similar findings with hepatic CYP3A (Fig. 10A), and the commonly observed ceiling to maximal P450 inducibility even after prolonged exposure to a given inducer, suggest that HRI plays a role in coordinating the heme and protein

[3] Although the exons corresponding to a functional eIF2α kinase HRI domain are genetically deleted in these C57BL/6J mice, an unstable defective HRI mRNA species may be transcribed that is detected by our HRI TaqMan probe.

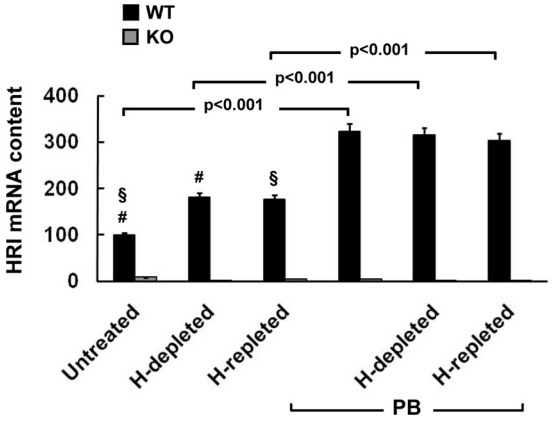

Fig. 11. qRT-PCR analyses of HRI mRNA after heme depletion or repletion of untreated or PB-treated C57BL/6J HRI (−/−; KO) hepatocytes and corresponding HRI (+/+; WT) controls. For experimental details, see *Materials and Methods*. Statistically significant differences were observed between the two mean ± S.D. values from 3 separate experiments each marked with the same symbol as follows: #, $p < 0.001$; §, $p < 0.001$; or as shown.

[4] This is inferred from our findings in Fig. 1A, wherein the immunochemically detectable HRI content of 10 μg of protein lysates of blood containing at best ≈1 to 2% reticulocytes was considerably higher than that of 100 μg of hepatocyte lysate protein. This possibility is consistent with the finding that a 60-fold greater amount of partially purified HRI-enriched liver protein than that of an erythroid HRI preparation, at the comparable stage of purification in an otherwise identical procedure, was required to inhibit protein synthesis by 50%, thereby also implying a greater HRI content per unit weight of reticulocyte than liver (Delaunay et al., 1977).

syntheses of hepatic P450s identical to that of its erythroid counterpart in hemoglobin synthesis (Chen, 2007).

We find it interesting that in mouse hepatocytes lacking HRI, the basal levels of total PERK, PERK-P, and/or GCN2 are significantly elevated over corresponding levels in the wild-type HRI(+/+) hepatocytes (Fig. 5), along with enhanced ubiquitination of total hepatic protein (Fig. 6A). Similar constitutive activation of eIF2α kinase activity was apparently also detected in HRI(−/−) murine embryonic fibroblasts (McEwen et al., 2005). These findings collectively reveal that hepatic HRI deletion leads to a significantly elevated basal cellular ER-stress tone, thereby suggesting that HRI may normally regulate this tone. Yet although GCN2 and PERK eIF2α kinases are secondarily activated after HRI deletion, it is intriguing that they fail to compensate for HRI in its absence by participating in translational control of PB-mediated P450 induction (Figs. 7 and 10A). Accordingly, despite the elevated cellular GCN2P, PERK-P, and eIF2αP levels in PB-treated HRI(−/−) hepatocytes (Figs. 8, 9, A and B, and 12B), PB-mediated P450 protein induction continues unabated, irrespective of whether the hepatic heme pool is depleted or repleted (Fig. 10A). Thus, of the four known eIF2α kinases, HRI seems to be the major eIF2α kinase involved in the heme-mediated translational control of CYP2B and CYP3A and possibly other hepatic P450s.[5] In this role, its hallmark heme-sensing capacity, not shared by the other eIF2α kinases, may be instrumental.

[5] We find it intriguing that, by contrast, proteasomal inhibitor MG132-mediated PERK induction/autophosphorylation indeed resulted in translational arrest of Dex-inducible CYP3A in rat hepatocytes containing normal levels of both HRI and heme (Acharya et al., 2009).

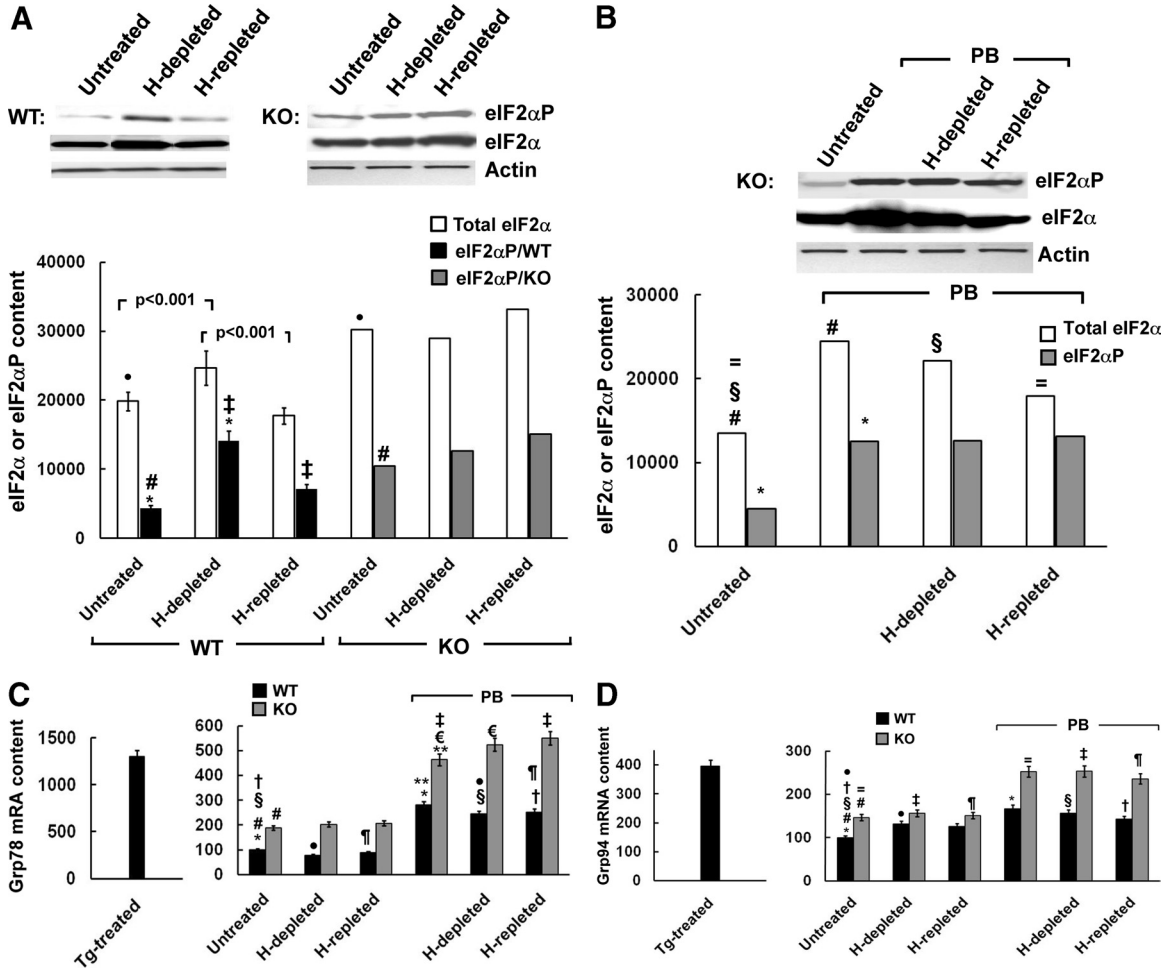

Fig. 12. The relative hepatic content of eIF2α and eIF2αP and qRT-PCR analyses of Grp78 and Grp 94 mRNA content in untreated and PB-treated C57BL/6J WT and HRI(−/−) hepatocytes. A, lysates from H-depleted or H-repleted hepatocytes were assayed exactly as detailed under *Materials and Methods*. A prototype immunoblot is shown. Values from C57BL/6J WT are mean ± S.D. of three separate experiments or average of two separate experiments in the case of the C57BL/6J HRI (−/−). The interindividual variability between the two average values of two separate experiments each marked by the same symbol was >10%. B, hepatocytes were treated exactly as detailed under *Materials and Methods*. Lysates from H-depleted or H-repleted hepatocytes were assayed exactly as detailed in Fig. 8B. A prototype immunoblot is shown. The interindividual variability between the two average values of two separate experiments each marked by the same symbol was >10%. C, qRT-PCR analyses of Grp78 mRNA after heme depletion or repletion of untreated or PB-treated C57BL/6J HRI (−/−; KO) hepatocytes and corresponding HRI (+/+; WT) controls. Corresponding analyses of Grp78 mRNA from hepatocytes treated in parallel with thapsigargin (Tg), an established ER-stress inducer, are also included. Note the *Y*-axes scale differences. For experimental details, see *Materials and Methods*. Statistically significant differences were observed between the two mean ± S.D. values from three separate experiments each marked with the same symbol as follows: #, $p < 0.05$; §, $p < 0.001$; ‡, $p < 0.05$; ¶, $p < 0.001$; €, $p < 0.05$; =, $p < 0.001$; ●, $p < 0.001$; †, $p < 0.001$; ∗, $p < 0.05$; and ∗∗, $p < 0.001$. D, corresponding qRT-PCR analyses of Grp94 mRNA. Statistically significant differences between the two mean ± S.D. values from three separate experiments each marked with the same symbol were as follows: #, $p < 0.05$; §, $p < 0.05$; ‡, $p < 0.001$; ¶, $p < 0.001$; =, $p < 0.05$; ●, $p < 0.05$; †, $p < 0.05$; and ∗, $p < 0.05$.

On the other hand, the significantly elevated mRNA and protein levels of the ER chaperones Grp78 and Grp94 in HRI(−/−) over HRI(+/+) hepatocytes, coupled with the elevated PERK and GCN2 eIF2α kinase autoactivation, suggest that hepatic heme pool perturbation of HRI-deficient cells elicits ER stress-counteractive responses (Figs. 6, B and C, 9, C and D, and 12, C and D). However, albeit statistically significant, these Grp increases are relatively small compared with those triggered by thapsigargin, a well known ER-stress inducer (Fig. 12, C and D), thereby signaling a relatively weak cellular ER stress response.

Our findings also reveal marked differences in the constitutive activation of HRI in mouse, rat, and human hepatocytes. Freshly isolated cells from human, rat, and C57BL/6J mouse liver predominantly, if not solely, contain HRI in its native unphosphorylated latent state (≈76 kDa) that is apparently heme-sensitive (Fig. 1A). Upon 5 days of culture, however, a small fraction of C57BL/6J mouse hepatic HRI, but not human or rat hepatic HRI, becomes constitutively autophosphorylated (Fig. 1, A and B). By contrast, HRI in freshly isolated BALB/c or MGB HRI(+/+) hepatocytes constitutively exists largely as its autoactivated/autophosphorylated 92-kDa (HRI-P) species (Fig. 1A), which is apparently heme-insensitive in vivo (Fig. 4). Intriguingly, purified recombinant mouse liver HRI also exhibits this characteristic ≈92-kDa retention on SDS-PAGE analyses, but its eIF2α kinase activity apparently remains inhibitable by hemin in vitro (IC_{50}, 0.5–9.5 μM; Chefalo et al., 1998; Berlanga et al., 1998; Miksanova et al., 2006; Igarashi et al., 2008). Our findings of the relative insensitivity of HRI eIF2α kinase to heme in MGB HRI(+/+) and BALB/c mouse hepatocytes in vivo (Fig. 4), in striking contrast to that observed in C57BL/6J mouse and rat hepatocytes (Fig. 2A; Liao et al., 2007), indicate that the native, nonphosphorylated HRI species is the most susceptible to heme inhibition in vivo, as previously found in vitro (Rafie-Kolpin et al., 2003). This may explain not only the poor HRI responsiveness to hepatic heme modulation in MGB HRI(+/+) and BALB/c hepatocytes, the HRI of which is largely autophosphorylated (Fig. 1B), but also the observed restitution of HRI heme sensitivity in MGB HRI(+/+) hepatocytes (Fig. 7) after PB-mediated increase of the nonphosphorylated 76-kDa HRI species (Fig. 8A).

We believe our finding that HRI exists in human hepatocytes in its unphosphorylated, heme-inhibitable latent form is clinically relevant. In this form, it is susceptible to functional activation in acute heme-deficient states, particularly relevant to patients genetically predisposed to the acute hepatic porphyrias. Its primary role may be that of a heme sensor to shut off protein synthesis and conserve vital energy and nutrients as well as contain ER and oxidative stress during acute heme-deficient conditions. In this context, the significant 3- to 5-fold increase of hepatic HRI mRNA and protein content after PB treatment of HRI(+/+) hepatocytes is particularly noteworthy (Figs. 1E, 8A, and 11). P450 inducers such as PB are clinically notorious for precipitating acute attacks of hepatic porphyria in genetically susceptible persons (Anderson et al., 2005). Thus, a priori, such drugs are contraindicated in this patient population. A plausible mechanism of their porphyric action is that by inducing hepatic P450 proteins, the major consumers of hepatic heme, such drugs aggravate the inherent hepatic heme deficiency in

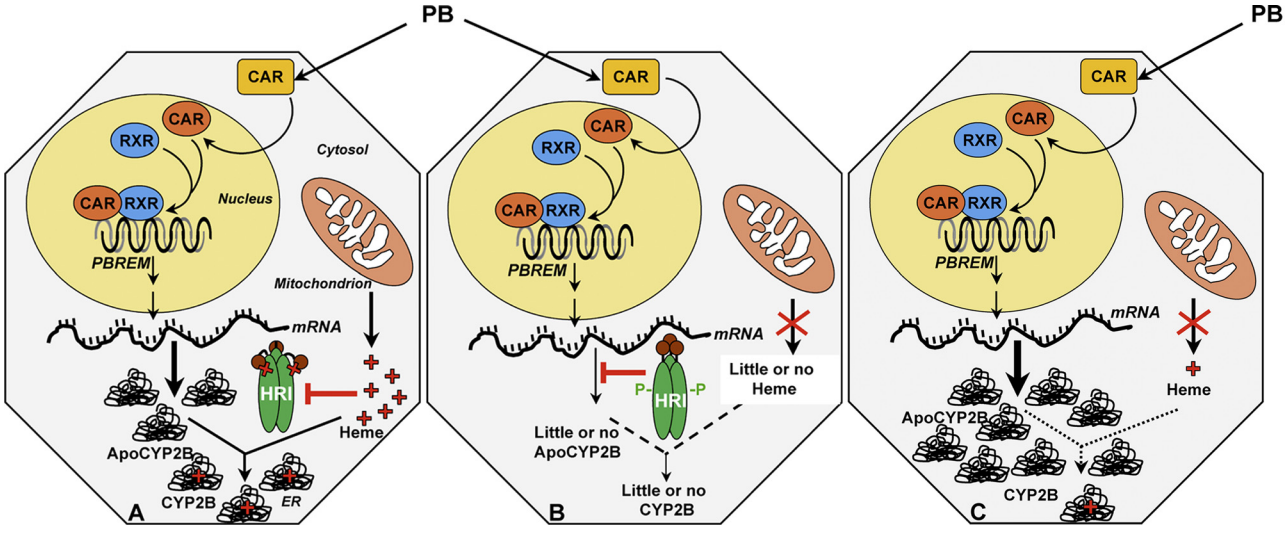

Fig. 13. Heme-mediated translational control of PB-mediated CYP2B induction via hepatic HRI. A, heme-repleted, C57BL/6J mouse HRI-WT hepatocytes. PB-mediated activation of cytoplasmic constitutive androstane receptor (CAR) results in its translocation into the nucleus, where it heterodimerizes with another nuclear receptor, retinoid X receptor (RXR). The CAR-RXR heterodimeric complex then interacts with the PB-responsive enhancer module (PBREM) in the 5′-promoter region of *CYP2B* genes, thereby inducing their expression through enhanced transcriptional-translational activation as detailed (Kim et al., 2001; Williams et al., 2004; Timsit and Negishi, 2007). PB induction of CYP2B protein requires coordinated induction of heme synthesis. Under conditions of normal hepatic heme availability, hepatic HRI is inhibited and functionally inactive, and CYP2B protein translation proceeds normally. After all available hepatic heme is consumed, the ensuing transient heme depletion would activate HRI, in turn shutting off CYP2B protein translation. B, heme-deficient, C57BL/6J mouse HRI-WT hepatocytes. Similar PB-mediated CAR-RXR transcriptional activation of *CYP2B* genes via PBREM occurs in the heme-deficient liver. In concurrence with previous reports (Srivastava et al., 1989; Sinclair et al., 1990; Jover et al., 2000), heme deficiency does not affect the transcriptional activation of *CYP2B* genes (Fig. 10B; Han et al., 2005b). However, heme deficiency relieves hepatic HRI from inhibition, resulting in its autoactivation (via autophosphorylation), thereby unleashing its eIF2α kinase activity with consequent arrest of global hepatic protein translation, including that of CYP2B enzymes. C, heme-deficient, HRI KO (−/−) mouse hepatocytes. Genetic deletion of HRI results in the loss of this translational control in response to heme deficiency. Consequently, after PB induction, uncontrolled de novo synthesis of hepatic proteins, including CYP2B, proceeds undeterred despite insufficient heme for holoP450 assembly. Inordinate accumulation of hepatic protein triggers enhanced ubiquitination and an ER stress response as discussed.

persons with genetic porphyria (De Matteis, 1978; Anderson et al., 2005). The marked increase in total and autoactivated/autophosphorylated hepatic HRI content by various P450 inducers (Figs. 1E and 8A) suggests that in addition to thus exacerbating hepatic heme deficiency, P450 inducers may also enhance translational control of key hepatic proteins. Indeed, hepatic HRI activation after acute hepatic heme depletion results in the translational shutoff of various hepatic proteins, including the ER-bound drug-metabolizing P450s and the cytosolic TDO, a key rate-limiting enzyme in tryptophan catabolism that determines the central and autonomic nervous systems serotonergic tone (Han et al., 2005b; Liao et al., 2007). Similar P450-inducer enhanced hepatic HRI activation, we believe, could play an active role in the translational arrest of a myriad of other physiologically relevant hepatic proteins during acute attacks of hepatic porphyrias and thus contribute to their often fatal clinical symptoms. Our qRT-PCR analyses reveal that this PB-mediated increase of hepatic HRI content involves a true induction of de novo HRI protein synthesis via increased transcription (Fig. 11). Whether this induction mechanism extends to the other HRI inducers (Fig. 1E) and/or involves stabilization of the existing protein is currently unknown. Nevertheless, our findings suggest that hepatic HRI may play a key role in the acute hepatic porphyrias. On the one hand, it is protective as a heme sensor, safeguarding cellular energy and nutrient resources during acute heme deficiency through translational control. On the other hand, it is insidious if its translational control were to extend to vital hepatic homeostatic functions, particularly in persons who are genetically predisposed. In sharp contrast, in murine models, its erythroid ortholog eHRI apparently serves largely a protective function by reducing the severity of erythropoietic protoporphyria as well as β-thalassemia through translational control (Han et al., 2005a).

In summary, our findings reveal that hepatic HRI is not only critical for heme-mediated translational regulation of PB-mediated hepatic P450 induction, but also for containing basal ER-stress. Its genetic deletion results in uncontrolled hepatic P450 protein synthesis as well as elevation of the basal ER-stress as reflected by the significantly elevated levels of autophosphorylated PERK and GCN2 eIF2α kinases, the ER-stress related chaperones Grp78 and Grp94, and total hepatic protein ubiquitination. Our findings that HRI is present in human hepatocytes in its native heme-inhibitable form that could be potentially activated in acute heme-deficient conditions such as the acute hepatic porphyrias indicate that they are clinically relevant.

Acknowledgments

We thank Ahalya Sriskandarajah (Department of Cellular and Molecular Pharmacology, University of California, San Francisco, CA) for valuable technical assistance and Roshini Zachariah, (Harvard-MIT Division of Health Sciences, MIT, Cambridge, MA), for confirmation of the HRI (+/+) and (−/−) mouse genotype. We also thank Prof. Ronald C. Wek (Indiana University, Indianapolis, IN) for providing a GCN2 antibody used in preliminary studies. We are grateful to Ali Naqvi, Theresa Canavan, and Chris Her (University of California San Francisco Liver Center Cell and Tissue Biology Core Facility, Dr. J. J. Maher, Director) for hepatocyte isolation and elutriation. We sincerely thank Dr. Mingxiang Liao for the preliminary studies that demonstrated eIF2α kinase activity in mouse hepatocytes. We also gratefully acknowledge Dr. Ed LeCluyse and Rachel Whisnant (CellzDirect/Invitrogen) for generously providing the human hepatocytes used in these studies. Finally, we are grateful to Dr. D. Montgomery Bissell (University of California, San Francisco) for critical review of this manuscript.

References

Acharya P, Engel JC, and Correia MA (2009) Hepatic CYP3A suppression by high concentrations of proteasomal inhibitors: a consequence of RNA-dependent protein kinase-like ER-bound eukaryotic initiation factor 2alpha (eIF2alpha)-kinase (PERK) and general control nonderepressible-2 eIF2α kinase (GCN2), and global translational shutoff. *Mol Pharmacol* **76:**503–515.

Anderson KE, Bloomer JR, Bonkovsky HL, Kushner JP, Pierach CA, Pimstone NR, and Desnick RJ (2005) Recommendations for the diagnosis and treatment of the acute porphyrias. *Ann Intern Med* **142:**439–450.

Berlanga JJ, Herrero S, and de Haro C (1998) Characterization of the hemin-sensitive eukaryotic initiation factor 2alpha kinase from mouse nonerythroid cells. *J Biol Chem* **273:**32340–32346.

Chefalo PJ, Oh J, Rafie-Kolpin M, Kan B, and Chen JJ (1998) Heme-regulated eIF-2alpha kinase purifies as a hemoprotein. *Eur J Biochem* **258:**820–830.

Chen JJ, Crosby JS, and London IM (1994) Regulation of heme-regulated eIF-2 alpha kinase and its expression in erythroid cells. *Biochimie* **76:**761–769.

Chen JJ (2000) Heme-regulated eIF-2α kinase, in *Translational Control of Gene Expression* (Sonenberg N, Hershey JWB, Mathews MB eds) pp 529–546, Cold Spring Harbor Laboratory Press, Cold Spring Harbor, NY.

Chen JJ (2007) Regulation of protein synthesis by the heme-regulated eIF2alpha kinase: relevance to anemias. *Blood* **109:**2693–2699.

Correia MA, Sadeghi S, and Mundo-Paredes E (2005) Cytochrome P450 ubiquitination: branding for the proteolytic slaughter? *Annu Rev Pharmacol Toxicol* **45:**439–464.

Crosby JS, Lee K, London IM, and Chen JJ (1994) Erythroid expression of the heme-regulated eIF-2 alpha kinase. *Mol Cell Biol* **14:**3906–3914.

De Matteis F (1978) Hepatic porphyrias. *Handb Exp Pharmacol* **44:**129–155.

Delaunay J, Ranu RS, Levin DH, Ernst V, and London IM (1977) Characterization of a rat liver factor that inhibits initiation of protein synthesis in rabbit reticulocyte lysates. *Proc Natl Acad Sci U S A* **74:**2264–2268.

Faouzi S, Medzihradszky KF, Hefner C, Maher JJ, and Correia MA (2007) Characterization of the physiological turnover of native and inactivated cytochromes P450 3A in cultured rat hepatocytes: a role for the cytosolic AAA ATPase p97? *Biochemistry* **46:**7793–7803.

Han AP, Fleming MD, and Chen JJ (2005a) Heme-regulated eIF2alpha kinase modifies the phenotypic severity of murine models of erythropoietic protoporphyria and beta-thalassemia. *J Clin Invest* **115:**1562–1570.

Han AP, Yu C, Lu L, Fujiwara Y, Browne C, Chin G, Fleming M, Leboulch P, Orkin SH, and Chen JJ (2001) Heme-regulated eIF2alpha kinase (HRI) is required for translational regulation and survival of erythroid precursors in iron deficiency. *EMBO J* **20:**6909–6918.

Han XM, Lee G, Hefner C, Maher JJ, and Correia MA (2005b) Heme-reversible impairment of CYP2B1/2 induction in heme-depleted rat hepatocytes in primary culture: translational control by a hepatic α-subunit of the eukaryotic initiation factor kinase? *J Pharmacol Exp Ther* **314:**128–138.

Harding HP, Calfon M, Urano F, Novoa I, and Ron D (2002) Transcriptional and translational control in the Mammalian unfolded protein response. *Annu Rev Cell Dev Biol* **18:**575–599.

Harding HP, Zhang Y, Zeng H, Novoa I, Lu PD, Calfon M, Sadri N, Yun C, Popko B, Paules R, et al. (2003) An integrated stress response regulates amino acid metabolism and resistance to oxidative stress. *Mol Cell* **11:**619–633.

Igarashi J, Murase M, Iizuka A, Pichierri F, Martinkova M, and Shimizu T (2008) Elucidation of the heme binding site of heme-regulated eukaryotic initiation factor 2alpha kinase and the role of the regulatory motif in heme sensing by spectroscopic and catalytic studies of mutant proteins. *J Biol Chem* **283:**18782–18791.

Igarashi J, Sato A, Kitagawa T, Yoshimura T, Yamauchi S, Sagami I, and Shimizu T (2004) Activation of heme-regulated eukaryotic initiation factor 2alpha kinase by nitric oxide is induced by the formation of a five-coordinate NO-heme complex: optical absorption, electron spin resonance, and resonance raman spectral studies. *J Biol Chem* **279:**15752–15762.

Jover R, Hoffmann F, Scheffler-Koch V, and Lindberg RL (2000) Limited heme synthesis in porphobilinogen deaminase-deficient mice impairs transcriptional activation of specific cytochrome P450 genes by phenobarbital. *Eur J Biochem* **267:**7128–7137.

Kaufman RJ (2004) Regulation of mRNA translation by protein folding in the endoplasmic reticulum. *Trends Biochem Sci* **29:**152–158.

Kim J, Min G, and Kemper B (2001) Chromatin assembly enhances binding to the CYP2B1 phenobarbital-responsive unit (PBRU) of nuclear factor-1, which binds simultaneously with constitutive androstane receptor (CAR)/retinoid X receptor (RXR) and enhances CAR/RXR-mediated activation of the PBRU. *J Biol Chem* **276:**7559–7567.

LeCluyse E, Bullock P, Madan A, Carroll K, and Parkinson A (1999) Influence of extracellular matrix overlay and medium formulation on the induction of cytochrome P-450 2B enzymes in primary cultures of rat hepatocytes. *Drug Metab Dispos* **27:**909–915.

Liao M, Pabarcus MK, Wang Y, Hefner C, Maltby DA, Medzihradszky KF, Salas-Castillo SP, Yan J, Maher JJ, and Correia MA (2007) Impaired dexamethasone-mediated induction of tryptophan 2,3-dioxygenase in heme-deficient rat hepatocytes: translational control by a hepatic eIF2alpha kinase, the heme-regulated inhibitor. *J Pharmacol Exp Ther* **323:**979–989.

Lu L, Han AP, and Chen JJ (2001) Translation initiation control by heme-regulated

eukaryotic initiation factor 2alpha kinase in erythroid cells under cytoplasmic stresses. *Mol Cell Biol* **21:**7971–7980.
McEwen E, Kedersha N, Song B, Scheuner D, Gilks N, Han A, Chen JJ, Anderson P, and Kaufman RJ (2005) Heme-regulated inhibitor kinase-mediated phosphorylation of eukaryotic translation initiation factor 2 inhibits translation, induces stress granule formation, and mediates survival upon arsenite exposure. *J Biol Chem* **280:**16925–16933.
Mellor H, Flowers KM, Kimball SR, and Jefferson LS (1994) Cloning and characterization of cDNA encoding rat hemin-sensitive initiation factor-2 alpha (eIF-2 alpha) kinase. Evidence for multitissue expression. *J Biol Chem* **269:**10201–10204.
Miksanova M, Igarashi J, Minami M, Sagami I, Yamauchi S, Kurokawa H, and Shimizu T (2006) Characterization of heme-regulated eIF2alpha kinase: roles of the N-terminal domain in the oligomeric state, heme binding, catalysis, and inhibition. *Biochemistry* **45:**9894–9905.
Pal JK, Chen JJ, and London IM (1991) Tissue distribution and immunoreactivity of heme-regulated eIF-2 alpha kinase determined by monoclonal antibodies. *Biochemistry* **30:**2555–2562.
Pascual M, Gómez-Lechón MJ, Castell JV, and Jover R (2008) ATF5 is a highly abundant liver-enriched transcription factor that cooperates with constitutive androstane receptor in the transactivation of CYP2B6: implications in hepatic stress responses. *Drug Metab Dispos* **36:**1063–1072.
Rafie-Kolpin M, Han AP, and Chen JJ (2003) Autophosphorylation of threonine 485 in the activation loop is essential for attaining eIF2alpha kinase activity of HRI. *Biochemistry* **42:**6536–6544.
Scheuner D, Patel R, Wang F, Lee K, Kumar K, Wu J, Nilsson A, Karin M, and Kaufman RJ (2006) Double-stranded RNA-dependent protein kinase phosphorylation of the alpha-subunit of eukaryotic translation initiation factor 2 mediates apoptosis. *J Biol Chem* **281:**21458–21468.
Sinclair PR, Schuetz EG, Bement WJ, Haugen SA, Sinclair JF, May BK, Li D, and Guzelian PS (1990) Role of heme in phenobarbital induction of cytochromes P450 and 5-aminolevulinate synthase in cultured rat hepatocytes maintained on an extracellular matrix. *Arch Biochem Biophys* **282:**386–392.
Srivastava G, Bawden MJ, Hansen AJ, and May BK (1989) Heme may not be a positive regulator of cytochrome-P450 gene expression. *Eur J Biochem* **178:**689–692.
Timsit YE and Negishi M (2007) CAR and PXR: the xenobiotic-sensing receptors. *Steroids* **72:**231–246.
Wek RC, Jiang HY, and Anthony TG (2006) Coping with stress: eIF2 kinases and translational control. *Biochem Soc Trans* **34:**7–11.
Williams SN, Dunham E, and Bradfield CA (2004) Induction of cytochrome P450 enzymes, in *Cytochrome P450: Structure, Mechanism, and Biochemistry*, 3rd ed (Ortiz de Montellano PR ed) pp 323–349, Kluwer Academic Press/Plenum, New York.
Zhang J, Socolovsky M, Gross AW, and Lodish HF (2003) Role of Ras signaling in erythroid differentiation of mouse fetal liver cells: functional analysis by a flow cytometry-based novel culture system. *Blood* **102:**3938–3946.
Zhang P, McGrath B, Li S, Frank A, Zambito F, Reinert J, Gannon M, Ma K, McNaughton K, and Cavener DR (2002a) The PERK eukaryotic initiation factor 2 alpha kinase is required for the development of the skeletal system, postnatal growth, and the function and viability of the pancreas. *Mol Cell Biol* **22:**3864–3874.
Zhang P, McGrath BC, Reinert J, Olsen DS, Lei L, Gill S, Wek SA, Vattem KM, Wek RC, Kimball SR, et al. (2002b) The GCN2 eIF2alpha kinase is required for adaptation to amino acid deprivation in mice. *Mol Cell Biol* **22:**6681–6688.

Address correspondence to: M. A. Correia, Dept. of Cellular and Molecular Pharmacology, Mission Bay Campus, Genentech Hall, 600 16th Street, N572F/Box 2280, University of California, San Francisco, CA 94158. E-mail: almira.correia@ucsf.edu